Titre: Title:	Roadmap on metasurfaces
Auteurs: Authors:	Oscar Quevedo-Teruel, Hongsheng Chen, Ana Díaz-Rubio, Gurkan Gok, Anthony Grbic, Gabriele Minatti, Enrica Martini, Stefano Maci, George V. Eleftheriades, Michael Chen, Nikolay I. Zheludev, Nikitas Papasimakis, Sajid Choudhury, Zhaxylyk A. Kudyshev, Soham Saha, Harsha Reddy, Alexandra Boltasseva, Vladimir M. Shalaev, Alexander V. Kildishev, Daniel Sievenpiper, Christophe Caloz, Andrea Alù, Qiong He, Lei Zhou, Guido Valerio, Eva Rajo-Iglesias, Zvonimir Sipus, Francisco Mesa, Raul Rodríguez-Berral, Francisco Medina, Victor Asadchy, Sergei Tretyakov, & Christophe Craeye
Date:	2019
Type:	Article de revue / Article
Référence: Citation:	Quevedo-Teruel, O., Chen, H., Díaz-Rubio, A., Gok, G., Grbic, A., Minatti, G., Martini, E., Maci, S., Eleftheriades, G. V., Chen, M., Zheludev, N. I., Papasimakis, N., Choudhury, S., Kudyshev, Z. A., Saha, S., Reddy, H., Boltasseva, A., Shalaev, V. M., Kildishev, A. V., ... Craeye, C. (2019). Roadmap on metasurfaces. Journal of Optics, 21(7), 073002 (44 pages). https://doi.org/10.1088/2040-8986/ab161d

Titre de la revue: Journal Title:	Journal of Optics (vol. 21, no. 7)
Maison d'édition: Publisher:	IOP Science
URL officiel: Official URL:	https://doi.org/10.1088/2040-8986/ab161d

Journal of Optics

ROADMAP • **OPEN ACCESS**

Roadmap on metasurfaces

To cite this article: Oscar Quevedo-Teruel *et al* 2019 *J. Opt.* **21** 073002

OPEN ACCESS

Made open access 14 August 2019

IOP Publishing

Journal of Optics

J. Opt. **21** (2019) 073002 (44pp)

https://doi.org/10.1088/2040-8986/ab161d

Roadmap

Roadmap on metasurfaces

Oscar Quevedo-Teruel[1,20,21], Hongsheng Chen[2,20], Ana Díaz-Rubio[3,20], Gurkan Gok[4], Anthony Grbic[5], Gabriele Minatti[6], Enrica Martini[6], Stefano Maci[6], George V Eleftheriades[7], Michael Chen[7], Nikolay I Zheludev[8,9], Nikitas Papasimakis[8,9], Sajid Choudhury[10], Zhaxylyk A Kudyshev[10], Soham Saha[10], Harsha Reddy[10], Alexandra Boltasseva[10], Vladimir M Shalaev[10], Alexander V Kildishev[10], Daniel Sievenpiper[11], Christophe Caloz[12], Andrea Alù[13], Qiong He[14], Lei Zhou[14], Guido Valerio[15], Eva Rajo-Iglesias[16], Zvonimir Sipus[17], Francisco Mesa[18], Raul Rodríguez-Berral[18], Francisco Medina[18], Victor Asadchy[3], Sergei Tretyakov[3] and Christophe Craeye[19]

[1] KTH Royal Institute of Technology, Stockholm, Sweden
[2] Zhejiang University, People's Republic of China
[3] Department of Electronics and Nanoengineering, Aalto University, PO 15500, FI-00076, Aalto, Finland
[4] United Technologies Research Center, East Hartford, CT, United States of America
[5] Department of Electrical Engineering and Computer Science, University of Michigan, Ann Arbor, MI, United States of America
[6] Dipartimento di Ingegneria dell'Informazione e Scienze Matematiche, University of Siena, 53100 Siena, Italy
[7] Department of Electrical and Computer Engineering, University of Toronto, Canada
[8] University of Southampton, Southampton, United Kingdom
[9] Nanyang Technological University, Singapore
[10] School of Electrical & Computer Engineering and Birck Nanotechnology Center, Purdue University, West Lafayette, IN 47907, United States of America
[11] University of California, San Diego, CA, United States of America
[12] Polytechnique Montréal, Canada
[13] Photonics Initiative, Advanced Science Research Center, City University of New York, New York, United States of America
[14] State Key Laboratory of Surface Physics and Physics Department, Fudan University, Shanghai 200433, People's Republic of China
[15] Laboratoire d'Electronique et Electromagnétisme, Sorbonne Université Paris, Paris, France
[16] University Carlos III of Madrid, Madrid, Spain
[17] Faculty of Electrical Engineering and Computing, University of Zagreb, Zagreb, Croatia
[18] University of Seville, Seville, Spain
[19] Université Catholique de Louvain, Belgium

E-mail: oscarqt@kth.se, hansomchen@zju.edu.cn and ana.diazrubio@aalto.fi

Received 12 October 2018, revised 19 December 2018
Accepted for publication 4 April 2019
Published 1 July 2019

Abstract

Metasurfaces are thin two-dimensional metamaterial layers that allow or inhibit the propagation of electromagnetic waves in desired directions. For example, metasurfaces have been demonstrated to produce unusual scattering properties of incident plane waves or to guide and modulate surface waves to obtain desired radiation properties. These properties have been employed, for example, to create innovative wireless receivers and transmitters. In addition,

[20] Guest Editors of the Roadmap.
[21] Author to whom any correspondence should be addressed.

metasurfaces have recently been proposed to confine electromagnetic waves, thereby avoiding undesired leakage of energy and increasing the overall efficiency of electromagnetic instruments and devices. The main advantages of metasurfaces with respect to the existing conventional technology include their low cost, low level of absorption in comparison with bulky metamaterials, and easy integration due to their thin profile. Due to these advantages, they are promising candidates for real-world solutions to overcome the challenges posed by the next generation of transmitters and receivers of future high-rate communication systems that require highly precise and efficient antennas, sensors, active components, filters, and integrated technologies. This Roadmap is aimed at binding together the experiences of prominent researchers in the field of metasurfaces, from which explanations for the physics behind the extraordinary properties of these structures shall be provided from viewpoints of diverse theoretical backgrounds. Other goals of this endeavour are to underline the advantages and limitations of metasurfaces, as well as to lay out guidelines for their use in present and future electromagnetic devices.

This Roadmap is divided into five sections:

1. **Metasurface based antennas.** In the last few years, metasurfaces have shown possibilities for advanced manipulations of electromagnetic waves, opening new frontiers in the design of antennas. In this section, the authors explain how metasurfaces can be employed to tailor the radiation properties of antennas, their remarkable advantages in comparison with conventional antennas, and the future challenges to be solved.
2. **Optical metasurfaces.** Although many of the present demonstrators operate in the microwave regime, due either to the reduced cost of manufacturing and testing or to satisfy the interest of the communications or aerospace industries, part of the potential use of metasurfaces is found in the optical regime. In this section, the authors summarize the classical applications and explain new possibilities for optical metasurfaces, such as the generation of superoscillatory fields and energy harvesters.
3. **Reconfigurable and active metasurfaces.** Dynamic metasurfaces are promising new platforms for 5G communications, remote sensing and radar applications. By the insertion of active elements, metasurfaces can break the fundamental limitations of passive and static systems. In this section, we have contributions that describe the challenges and potential uses of active components in metasurfaces, including new studies on non-Foster, parity-time symmetric, and non-reciprocal metasurfaces.
4. **Metasurfaces with higher symmetries.** Recent studies have demonstrated that the properties of metasurfaces are influenced by the symmetries of their constituent elements. Therefore, by controlling the properties of these constitutive elements and their arrangement, one can control the way in which the waves interact with the metasurface. In this section, the authors analyze the possibilities of combining more than one layer of metasurface, creating a higher symmetry, increasing the operational bandwidth of flat lenses, or producing cost-effective electromagnetic bandgaps.
5. **Numerical and analytical modelling of metasurfaces.** In most occasions, metasurfaces are electrically large objects, which cannot be simulated with conventional software. Modelling tools that allow the engineering of the metasurface properties to get the desired response are essential in the design of practical electromagnetic devices. This section includes the recent advances and future challenges in three groups of techniques that are broadly used to analyze and synthesize metasurfaces: circuit models, analytical solutions and computational methods.

Keywords: metasurfaces, two-dimensional metamaterials, antennas, high-rate communications

(Some figures may appear in colour only in the online journal)

Contents

METASURFACE BASED ANTENNAS

1. Tailoring aperture fields with metasurfaces

Gurkan Gok[1] *and Anthony Grbic*[2]

[1]United Technologies Research Center, East Hartford, CT, United States of America
[2]Department of Electrical Engineering and Computer Science, University of Michigan, Ann Arbor, MI, United States of America

Status. Tailoring aperture fields in phase, amplitude and polarization is the key aim of versatile antenna systems. An aperture's amplitude and phase characteristics govern the beam shape, beam pointing direction, and beam polarization. Traditionally, aperture fields of high gain microwave and millimeter-wave antennas have been established by reflectors/lenses excited by simple feed antennas (e.g. dish antennas, lens antennas, reflectarrays, transmitarrays), and steered by mechanical means. This conventional approach results in large and heavy structures, due the bulky reflectors/lenses, gimbals and displaced feed antennas employed. Alternatively, apertures can be composed of discrete antenna elements, and electronically controlled, as in the case of phased arrays. Phased arrays, however, are costly and exhibit high feed network losses that grow with aperture size and frequency.

Recent developments in metasurfaces have opened new opportunities in antenna design. Metasurfaces are surfaces textured at a subwavelength scale to achieve tailored electromagnetic surface properties. They hold promise for the development of low cost, light weight, and compact antennas capable of producing arbitrary aperture fields. Metasurfaces transform wavefronts by imparting field discontinuities across their thin and potentially electrically large and/or conformal surfaces. Their ability to control wavefronts through texture allows for the separation of geometry from electromagnetic functionality. Thus, metasurfaces can take on various form factors, while controlling waves through their subwavelength pattern/granularity. This is in contrast to traditional lenses, which control waves through geometry/shape.

Metasurface antennas can transform fields of a source excitation into an arbitrary radiating aperture field, either by judiciously guiding waves toward an aperture that radiates, or by supporting leaky-waves that directly radiate targeted radiation patterns. In [1], anisotropy and inhomogeneity were exploited to transform a source field into a complex (phase and amplitude) aperture through the manipulation of the phase and power flow of guided waves, allowing independent control of an aperture's phase and amplitude distributions. Various one-dimensional aperture profiles, in phase and amplitude, were theoretically demonstrated [1]. The approach was used to demonstrate beamformer antennas implemented using transmission-line based metamaterials possessing anisotropic material properties and a true-time-delay response [2]. The beamformers achieved beam scanning through a lateral displacement of its feed. The approach was later extended to design aperture antennas that can excite tailored (aberration free) beams for displaced feed locations [3] (see figure 1(a)). Simulated radiation efficiencies over 30% were reported between 10 GHz and 13 GHz for beam scanning between ±30°, in 10° steps. Beam pointing directions remained constant over the operational band due to the true-time-delay behavior of the design. Coupling between feedlines degraded antenna patterns below 10 GHz. Analogously, cascaded metasurfaces have been recently reported that can create complex aperture fields with arbitrary phase and amplitude profiles through sequential, lossless and reciprocal phase manipulation [4].

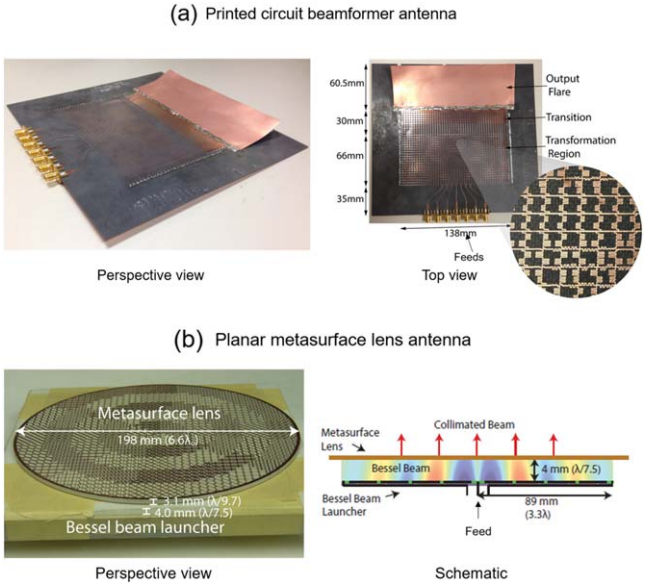

Figure 1. Metasurface antennas can transform fields of a source excitation into arbitrary radiating aperture fields either by (a) guiding them towards an aperture that radiates [3], or (b) supporting traveling/leaky-waves that radiate directive radiation patterns [7]. (a) © 2018 IEEE. Reprinted, with permission, from [3]. (b) © 2015 IEEE. Reprinted, with permission from [7].

There has also been significant activity in the development of traveling-wave metasurface antennas [5]. In addition, metasurface-based lenses that are directly integrated with feed antennas have been reported [6]. Such lens-based antennas have demonstrated an order of magnitude reduction in thickness compared to traditional lens-based antennas [7] (see figure 1(b)). An experimental lens-antenna system operating at 9.9 GHz with approximate radiation efficiency of 50%, aperture efficiency of 70%, half-power gain bandwidth around 8%, and impedance bandwidth of around 4% was reported [7]. The low-profile metasurface lens antenna was designed by cascading two functional metasurfaces over a radial cavity. The first metasurface supports a cylindrical leaky-wave which illuminates the second metasurface. The second metasurface, phase and polarization correct

the emitted radiation, creating directive radiation patterns of linear or circular polarization. The two metasurfaces essentially form an asymmetric (bianisotropic) metasurface that allows one to tailor the reflected and transmitted phase, as well as transmission/reflection amplitude. Such an approach demonstrated a path towards modular antenna design, where layers of metasurfaces are cascaded to tailor the aperture of directly-fed, low-profile antennas. The approach eliminates the displaced feed typically used in lens and reflector antennas. Single metasurfaces above a thin cavity have also been reported that tailor cavity modes into arbitrary aperture fields [8, 9]. These extremely low-profile, high gain antennas that employ a single metasurface with bianisotropic properties have demonstrated precise control of radiation patterns.

Current and future challenges. Although metasurface-based antennas show great promise for dramatically reducing the size and complexity of antenna systems, certain challenges lie ahead for their mass deployment. Metasurfaces consist of subwavelength resonators with electromagnetic properties that are often times frequency dispersive. In other words, the resonant nature of a metasurface's constitutive elements can restrict the usable bandwidth of metasurface-based antennas. Single layer metasurface antennas with operational bandwidths of up to 8% have been reported [7, 8, 10]. In comparison, a commercially available Ku-band SATCOM antenna covers global receive and transmit bands nearing a total bandwidth of 23%. Furthermore, if simultaneous operation in multiple satellite communication bands is desired with a single antenna, even larger bandwidths or multiband performance [11] are needed.

Electrically addressable/reconfigurable metasurfaces pose further challenges. High gain antennas with dynamic beam steering are often needed/desired in wireless applications ranging from satellite, 5G communications to remote sensing, imaging and radar. The introduction of tunability can limit performance (increase loss, limit bandwidth, etc) and result in complex control (tuning, biasing, etc) circuitry. Mechanisms such as externally controllable circuit components (varactors, pin diodes) [12] and liquid crystal layers [13] have been investigated for dynamic reconfigurability. Circuit-based approaches face scaling challenges in high gain metasurfaces. With increased size, the number of components dramatically increases, along with cost and losses, if deep subwavelength cell dimensions are maintained. Liquid crystal layers are scalable, and have shown promising results at mm-waves. However, they are relatively slow with millisecond response times. As for the complexity of the control circuitry, questions remain on how such circuitry can be incorporated without interfering with the microwave/millimeter wave performance of the metasurface.

Metasurfaces have provided antenna designers with an enhanced surface parameter set, but how does one exploit these added degrees of freedom to design a metasurface antenna with a specified aperture distribution? Transformation optics provides a systematic approach to tailoring radiating apertures [14, 15]. However, the approach has been limited to tailoring fields from a single elementary source.

Advances in science and technology to meet challenges. Improvements to the bandwidth of metasurface-based antennas can be made by combining the spatial field manipulation offered by metasurfaces with traditional filter concepts, in order to provide both spatial and spectral manipulation of fields. Maximally linear phase responses and true-time-delay responses have been achieved using filter concepts in lens-based antennas and reflectarrays [16, 17]. These approaches have shown to be effective at microwave frequencies. However, the multilayer fabrication needed to realize these metasurfaces becomes increasingly challenging at higher frequencies. It should also be noted that the broad bandwidths observed with transmissive or reflective metasurfaces have not translated to broadband, directly-fed metasurface-based antennas.

Advanced design techniques that integrate control circuitry into metasurface design, as well as the development of synthesis approaches for multi-input multi-output designs, can tackle some of the challenges associated with reconfigurable metasurfaces. Spatial light modulators use transparent conductors and thin film transistors to realize electrically addressable pixels/cells, but such transparent control circuitry is not available at microwave and millimeter-wave frequencies. Therefore, metasurface patterns at these frequencies must serve a dual purpose: provide the microwave/mm-wave surface properties needed, as well as incorporate the control/bias circuitry [18].

A synthesis technique for multi-input, multi-output metasurface devices (i.e. devices that are capable of transforming distinct source field distributions to distinct tailored beams) through compound metasurfaces (multiple cascaded metasurfaces) would allow a number of functionalities to be incorporated into a single device. Such an approach could remove the need for a reconfigurable mechanism for a finite number of functionalities. Towards this goal, a transformation medium that maps different excitations to specified output beams was recently designed through optimization, and reported in [4].

Concluding remarks. Metasurfaces provide new opportunities for the development of compact, low-cost and versatile antennas and quasi-optical systems. Although promising, performance and synthesis challenges, as well as tuning/reconfiguration mechanisms must be addressed before their use in antenna design becomes widespread. Metasurface antennas/radiators that are low-profile, low cost, fabricable over large areas, and offer extended capabilities could see wide scale deployment in various application areas ranging from terrestrial/satellite communication systems and aerial platforms, to radar and surveillance systems.

2. Modulated metasurface antennas

Gabriele Minatti, Enrica Martini and Stefano Maci

Dipartimento di Ingegneria dell'Informazione e Scienze Matematiche, University of Siena, Via Roma, 56 53100 Siena, Italy

Status. Modulated metasurface (MTS) antennas have emerged in the last ten years as a new concept of aperture antennas radiating by leaky-wave (LW) effect. The LW originates from a cylindrical wavefront surface-wave (SW) excited by a monopole and propagating on an MTS which imposes suitably modulated impedance boundary conditions (IBCs). Energy is leaked when the SW wavelength is properly matched to the local period of the periodic or quasi-periodic IBCs provided by the MTS. Through the MTS, amplitude, phase and polarization of the radiative field can be controlled to obtain desired radiation performance.

An MTS antenna is composed of a host medium with many small metallic or dielectric inclusions, often referred to as 'pixels', arranged in a regular lattice (figure 2). Due to the smaller losses, all-metallic technology is preferred to the printed dielectric technology at higher frequencies (above Ka-band). The SW is provided by a feeding system embedded in the MTS itself, which can be as simple as an elementary transverse magnetic (TM) radiator. The basic configuration of an MTS antenna therefore has a simple low profile structure. Amongst many, the most intriguing feature of MTS antennas is that performance can be easily tailored to a wide variety of application requirements, without significantly changing the fundamental structure. A simple modification of the global holography of the MTS leads to beam tilting, beam shaping, and polarization control. An example is shown in figure 3. This feature indeed opens the path to the research on dynamically adaptive MTS antennas which are able to steer or reconfigure the beam. The main concept is to dynamically change the IBCs offered by the MTS by acting on the inclusions composing the MTS through active devices or tunable materials.

Structures based on PCB layout are presently the most mature configuration for MTS antennas: the feasibility of the concept is well documented in literature (see, for instance, [19–22]) proving that the beam can be controlled in its shape, direction and polarization. A significant effort has been dedicated in recent years to develop effective design procedures, which now have reached a significant level of maturity [23]. The structural characteristics of these antennas are extremely appealing: MTS antennas are cost effective, easily manufactured with standard PCB techniques or 3D printing devices. They are light, low encumbrance and in principle conformable to different kinds of surfaces. These are intriguing features both for commercial and space applications (for which they were originally conceived [24]).

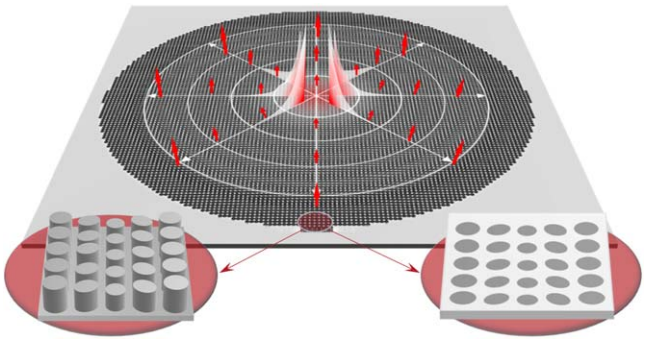

Figure 2. Metasurface antenna layout. An SW excited from the centre is gradually converted into a radiative LW by interacting with the MTS. At microwaves, the MTS is usually formed by a texture of printed patches on a grounded dielectric slab (right inset). Alternatively, usually at millimetre waves, the MTS can be formed by a tight distribution of metallic pins (left inset).

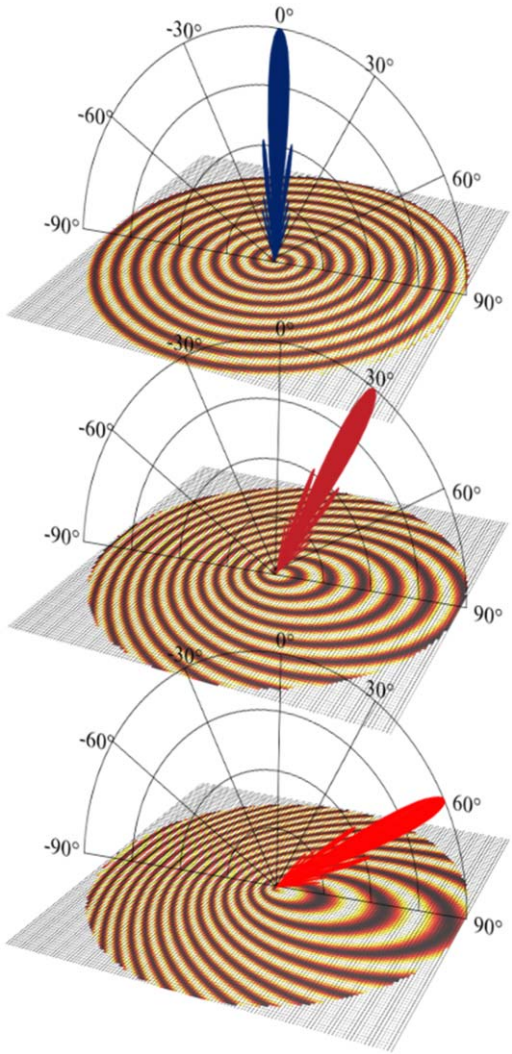

Figure 3. Dynamically adaptive MTS. By simply changing the IBCs offered by the MTS, the beam can be easily redirected without affecting the antenna structure.

Despite the MTS antenna concept being introduced a few years ago, there are still open issues. The most notable one is pattern bandwidth [25], i.e. pattern stability with respect to frequency, which is still a subject of concern. Pattern bandwidth is mainly limited by the mismatch between the SW wavelength and the periodicity of the IBCs occurring when the operational frequency changes from the design one. Instead, matching bandwidth, i.e. return loss bandwidth, is a minor limitation for the overall antenna bandwidth. Indeed, MTS antennas can be easily matched and, given the small size of the pixels, the MTS is far from resonance [24]. However, the performance in terms of the bandwidths of these antennas is quite robust with respect to alternative printed dipole technologies (i.e. patch array) with a simple feed point. Indeed, for constant average impedance MTS, with possibly non-uniform modulation index and uniform modulation period, the bandwidth is approximated by the simple formula

$$B \approx 0.95\frac{v_g}{c}\frac{1}{a_\lambda};\ \left(B \approx 1.2\frac{v_g}{c}\frac{1}{a_\lambda}\right) \tag{1}$$

where v_g is the group velocity of an SW propagating on the average impedance of the MTS, c is the speed of light in free space and a_λ is the radius in free-space wavelengths. The first equation in (1) is relevant to a uniform modulation of the IBC, while the equation in brackets is relevant to an optimized IBC modulation [25]. The corresponding expressions of the product bandwidth-gain are

$$BG \approx 22\frac{v_g}{c}a_\lambda;\ \left(BG \approx 47\frac{v_g}{c}\left[\frac{a_\lambda}{(a_\lambda+2)}\right]a_\lambda\right). \tag{2}$$

The above equations also establish physical limits in the product bandwidth-gain as $22a_\lambda$ ($47a_\lambda$). Better performance in terms of radiation-pattern bandwidth can be obtained by a non-uniform modulation period, namely by matching the local radial period of the modulation at different positions with the SW wavenumber at different frequencies. This leads to space-variable shapes of the holography conceptually similar to those obtained in spiral active region antennas. With this, one can enlarge the bandwidth to a wideband operation (till 25%), at the price of a significantly lower aperture efficiency. The performances of the bandwidths expressed in equations (1) and (2) are, however, suitable for many applications, including those for space, considering the fact that MTS antennas with more than 41 dBi of directivity have been recently measured in Ka-band.

Current and future challenges. Fast reconfigurability of the beam, beam scanning and multibeams are the most applicative impactful challenges today. Low-cost beam scanning antennas are particularly appealing for Sat-Com on the move and adapt well to the potential performance of the MTS technology. Fast beam hopping and multibeam operations with low power consumptions are interesting features for 5G applications. Overlapping apertures for multi-beaming are in fact already successfully devised for MTS antennas in static configuration, and exhibit promising potential on this concern. The possibility to easily customize the antenna feature in near field focusing also opens the door towards medical applications.

Dynamic, electronically reconfigurable MTS antennas need to be improved in terms of efficiency. The concept has already been demonstrated [26–28], where the inclusions of the MTS are loaded with active devices or they include liquid crystals or phase changing materials like vanadium dioxide. The electric features of the inclusions become voltage controlled and hence the IBCs offered by the MTS can be properly adjusted by an external control. Active devices or phase changing materials yield an increase of the antenna losses with a consequent reduction of gain and increase of power demand; losses become more important when working at higher frequencies (e.g. Ka-band): frequency scalability is indeed another future challenge. Also, phase changing materials suffer from temperature instability [29]. Alternative strategies make use of optical pumping of silicon or gallium arsenide substrates to alter the electrical properties of the inclusions. Losses become less critical when dealing with a mechanical reconfiguration. The use of micromechanical systems or piezoelectric devices have been proposed [30], but they may suffer from low reliability and an MTS antenna based on such devices may be too sensitive to the external vibrations if installed on moving vehicles.

Advances in science and technology to meet challenges. Despite the significant advances done in the framework of the design procedure [23], antenna optimization is still a future challenge topic. Whenever strong requirements on performance are demanded, it is necessary to optimize the final MTS layout which may be composed by up to a hundred thousand elements. Managing the high number of inclusions with numerical methods requires smart strategies which make combined use of homogenized boundary conditions and fast integral-equation solvers.

Extension of the MTS antenna concept to curved surfaces is a future challenge for conformable and aerodynamic applications. Meeting this challenge implies an extension of the creeping-wave theory to metasurface coated curved surfaces, which are almost absent at the present state of the art and would require a significant effort.

Advances in phase changing materials would bring a significant benefit to MTS antennas, in terms of losses and switching time reduction, as well as increase of temperature stability. Special liquid crystals for microwaves could be extremely beneficial, and some companies are investing in this direction. MTS with integrated active devices, instead of discrete active devices, would also bring advantages in terms of reliability, losses and performance. Realizing integrated devices on a wide area will require significant improvement of the accuracy and repeatability of the fabrication processes. 3D printing processes are also extremely appealing for MTS antennas, creating the possibility to move beyond the classical PCB processes, offering chances to build up the MTS, adding

specific features to the inclusions and hence improving performance with low-cost.

Concluding remarks. The operation principle of MTS antennas allows for tailoring the MTS with active devices, liquid crystals or phase changing materials in real time. While the initial concern of some time ago about bandwidth is a challenge in fast progress, losses, agility and dynamic speed are still open issues for both design and fabrication technology aspects. We have presented here challenges and perspectives of MTS antennas in the microwave domain. However, the operational principle behind SW control through MTS can be applied to a wide range of applications in nano-photonics and nanoengineering.

3. Huygens' metasurfaces for selected antenna applications

George V Eleftheriades and Michael Chen

Department of Electrical and Computer Engineering, University of Toronto, Canada

Status. Electromagnetic surfaces for antenna applications have a long history and include frequency-selective surfaces, transmit and reflect arrays, and more recently tensorial holographic surfaces [31]. Recently, metasurfaces have been introduced as 2D analogues of metamaterials [32]. Their unique characteristic is that these metasurfaces feature sub-wavelength unit cells, such that they can be homogenized with electric and magnetic surface susceptibilities or equivalent impedances and admittances. In this contribution, we will describe some recent advances of such metasurfaces for antenna applications.

Huygens' or 'field-discontinuity' metasurfaces when illuminated by an incident electromagnetic wave induce electric and magnetic dipole moments, which correspond to electric and magnetic surface current densities; see equation (3) [33, 34]. These currents, when properly excited, can shape the transmitted or reflected electromagnetic wave at will (see figure 4(a)).

$$\overline{\boldsymbol{J}}_s = \hat{\boldsymbol{n}} \times (\overline{\boldsymbol{H}}_2^+ - \overline{\boldsymbol{H}}_1^-),\ \overline{\boldsymbol{M}}_s = -\hat{\boldsymbol{n}} \times (\overline{\boldsymbol{E}}_2^+ - \overline{\boldsymbol{E}}_1^-). \qquad (3)$$

The challenge here is how to synthesize these surfaces so that the incident field can excite the required currents (3) to perform a desired field transformation. This can be aided by casting the problem in terms of spatially varying impedance and admittance sheets; see equations (4).

$$\overline{\boldsymbol{E}}_{t,avg} = \overline{\overline{\boldsymbol{Z}}}_{se} \cdot \overline{\boldsymbol{J}}_s - \overline{\overline{\boldsymbol{K}}}_{em} \cdot [\hat{\boldsymbol{n}} \times \overline{\boldsymbol{M}}_s] \qquad (4a)$$

$$\overline{\boldsymbol{H}}_{t,avg} = \overline{\overline{\boldsymbol{Y}}}_{sm} \cdot \overline{\boldsymbol{M}}_s - \overline{\overline{\boldsymbol{K}}}_{em} \cdot [\hat{\boldsymbol{n}} \times \overline{\boldsymbol{J}}_s]. \qquad (4b)$$

A natural embodiment of such Huygens' surfaces consists of an array of loaded strips and loops which can be tuned to synthesize the required surface reactances (4) (see figure 4(b)). In this way, such surfaces are conducive to antenna pattern shaping when illuminated by plane waves or by the fields from nearby elementary feeding sources.

To demonstrate the capability of these Huygens' metasurfaces (HMS), figures 4(c) and (d) show the case of reflectionless refraction of a normally incident plane wave at an extreme angle [35, 36]. This becomes possible because, on the one hand, the surface can excite both electric and magnetic dipole moments (3). On the other hand, these electric and magnetic dipole moments can be coupled together to provide a bi-anisotropic response as represented by the term $\overline{\overline{\boldsymbol{K}}}_{em}$ in (4) [37]. In this way, the angle-dependent impedance of the transmitted wave can be perfectly matched to the different impedance of the incident wave, with a passive and lossless surface.

A natural antenna application of these metasurfaces is for gain enhancement. A typical scenario is that of placing a low-directivity feeding antenna at the focal plane of a metasurface lens. In figure 5(a), we show the case of a cylindrical lens

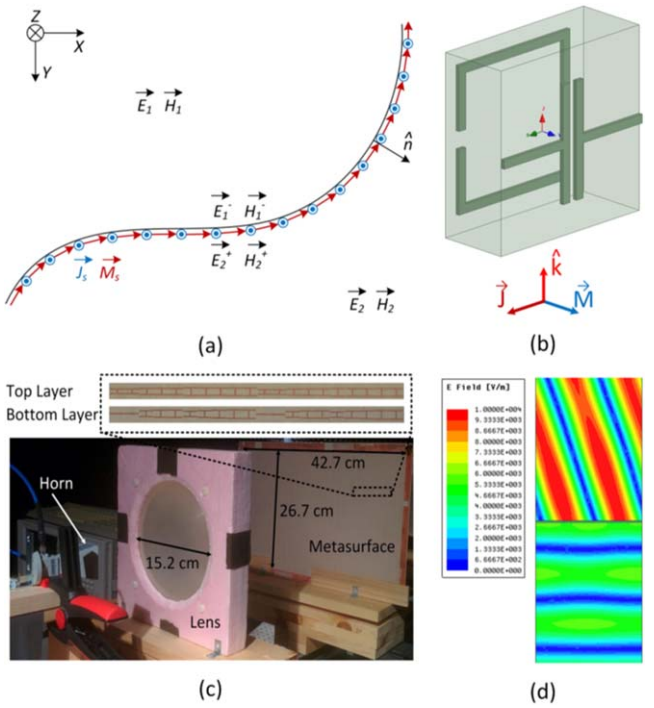

Figure 4. (a) The concept of a Huygens' metasurface [38]. (b) A loaded strip-loop unit cell [40]. (c) A reflectionless refracting bi-anisotropic metasurface tested using a quasi-optical system at 20 GHz [36]. (d) Full-wave simulation of reflectionless refraction for normal incidence to 71.8 degrees. (a) [38] 2018 Nature Communications. With permission of Springer. CC BY 4.0. (b) © 2017 IEEE. Reprinted, with permission, from [40]. (c) Reprinted figure with permission from [36], Copyright (2018) by the American Physical Society.

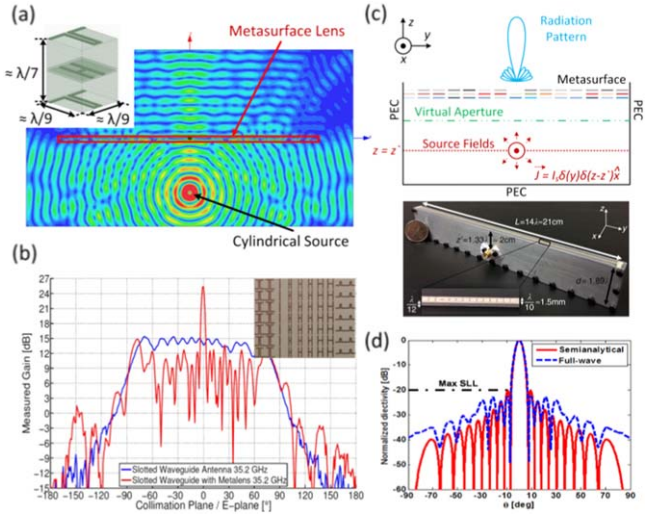

Figure 5. (a) A collimating Huygens' metasurface lens [39]. (Inset) A 'spider' unit cell has been used. (b) Beam collimation in the E-plane at 35.2 GHz [39]. (Inset) Top view of the metasurface metallization pattern. (c) Concept of a cavity excited metasurface to synthesize arbitrary antenna patterns [38]. (d) Synthesized one-parameter Taylor's distribution with sidelobes <-20 dB [40]. (a), (b) © 2018 IEEE. Reprinted, with permission, from [39]. (c) [38] 2018 Nature Communications. With permission of Springer. CC BY 4.0. (d) © 2017 IEEE. Reprinted, with permission, from [40].

antenna, implemented as a thin and flat Huygens' metasurface, to enhance the gain of a feeding slotted-waveguide antenna. For this, a 'spider' unit cell has been used, as shown in the inset of figure 5(a) [38]. The slotted waveguide exhibits a narrow beamwidth along the length of the guide (H-plane) but a wide beam along the transverse plane (E-plane). The metasurface lens placed in close proximity to the waveguide leaves the H-plane unchanged but collimates the E-plane considerably leading to an average gain enhancement of 10 dB around 35 GHz (see figure 5(b)) [39].

The advanced capability of these Huygens' metasurfaces is highlighted in the case of arbitrary antenna pattern synthesis. The general idea is to illuminate an HMS with an elementary pattern and transform this through the surface to an arbitrary antenna pattern. A possible embodiment of this concept is to embed an elementary feed antenna in an open cavity which is closed by a suitable HMS as shown in figure 5(c) [38]. The transmitted fields can be stipulated to correspond to a 'virtual array' with desired weights to synthesize a certain antenna pattern (in both magnitude and phase) [40]. The incident fields are a superposition of N cavity modes, each one characterized by a characteristic reflection coefficient $\mathbf{\Gamma}_n$. A bi-anisotropic HMS can be used to determine the reflection coefficients $\mathbf{\Gamma}_n$ such that local power conservation is achieved. The latter condition is required to ensure a metasurface that is passive and lossless (in principle). The reflection coefficients $\mathbf{\Gamma}_n$ can be determined using a suitable optimization algorithm. In this way, arbitrary antenna patterns, in terms of beamwidth and sidelobe structure, can be synthesized as shown in figure 5(d).

It should be understood that the method described above is in general applicable to other scenarios and not just for cavity excited metasurfaces. For example, one could envision a feed antenna exciting a pair of bi-anisotropic HMSs [41]. The fields in the region between the metasurfaces can be expanded in terms of N plane waves with weights $\mathbf{\Gamma}_n$ such that local power conservation is enforced, for a given desired excitation of the weights on the output 'virtual array'.

Current and future challenges

The versatility of the HMS has been highlighted in the previous section. In principle, these surfaces can manipulate at will the phase, magnitude and polarization (as implied by the general tensorial nature of (4)) of an incident wave. Despite this versatility, a challenge that remains is the difficulty to translate the spatially varying $\overline{\overline{\boldsymbol{Z}}}_{se}$, $\overline{\overline{\boldsymbol{Y}}}_{sm}$, $\overline{\overline{\boldsymbol{K}}}_{em}$ parameters in (4) using physical structures such as the wire-loop or other 3-metal-layer structures (see the inset in figure 5(a)). This can be a time-consuming process, requiring many trial and error steps to build a suitable geometry/material library for each physical platform. To address this challenge, dedicated electromagnetic CAD tools will need to be developed combined with suitable optimization routines. Another challenge that needs to be addressed directly is that of the bandwidth. To appreciate this, consider the simple example of a dielectric lens and its corresponding planar HMS implementation. The physical lens features extremely large bandwidth in terms of reflections and chromatic aberration (at least at microwave frequencies where dielectrics like glass have very little dispersion). However, typically HMSs will suffer from several effects that will limit their bandwidth. For example, at the cell level, there can be appreciable dispersion which would depart from the ideal frequency variation that is implied by (4) (typically corresponding to a linear transmission phase). Moreover, such HMS lenses would resemble zoned dielectric lenses, which would introduce additional frequency variation due to the zoning effect. This represents an opportunity for future development of broadband and/or multiband HMS [42]. Another challenge that opens up new opportunities is to render these metasurface antennas beam-scannable or, in general, reconfigurable. For this purpose, one can envision two possible avenues. The first would be to equip each constituent unit cell with simple electrically tunable element (s), such as varactors, transistors or even liquid crystals. This would alter their local impedance and achieve desired transformations in real time based on (4). However, the benefits and drawbacks of such an approach compared to traditional methods such as electronically scannable phased arrays should be carefully evaluated. The second avenue would be to use the metasurfaces as radomes, which are either fixed or of limited agility, above smaller phased arrays. In this way, the metasurface radome can be used to enhance the gain or the angular scan range of the underlying phased array [43].

OPTICAL METASURFACES

4. Metasurfaces beyond quasi-holography: creating unusual electromagnetic field structures in free-space

Nikolay I Zheludev and Nikitas Papasimakis

University of Southampton, Southampton, United Kingdom
Nanyang Technological University, Singapore

A few words about terminology and state of the art. The history of photonic metamaterials has largely been the history of metasurfaces, or planar metamaterials. Indeed, the majority of work on three-dimensional metamaterials has taken place in the microwave domain, where the fabrication of volume multi-layered structures is easier. Planar and quasi-planar metasurfaces have helped to observe a wide range of important effects including enhanced (nearly perfect) absolute absorption, giant linear and circular dichroism, negative index of refraction, Lorentz-reciprocity-compliant asymmetric transmission, toroidal dipole excitations and many other phenomena that are difficult or impossible to study in natural media.

However, in the current literature, the term 'metasurface' is predominantly used in relation to phenomena associated with wavefront modifications of electromagnetic radiation by diffraction on a planar metamaterial. Similarly to holography, the objective is to control the field structure in free space by appropriate patterning of a medium (metamaterial), which scatters electromagnetic radiation. Initial efforts in this research field involved the generation of radially and azimuthally polarized beams by space-variant dielectric subwavelength gratings [44] and the observation of polarization changes of light upon diffraction by gammadions assembled from metallic V-shaped elements [45]. The demonstrations of metasurface-based lenses [46] and wavevector selective metasurfaces, transparent only within a narrow range of light propagation directions operating as tunnel vision filters [47], also belong to this class of effects. The field of metasurfaces gained considerable prominence and massive follow-up after the demonstration of anomalous refraction on gradient metasurfaces [48] and the development of high-throughput metasurfaces for focusing of light [49].

Emerging applications of metasurfaces. New, interesting and important future directions for metasurfaces will go beyond mimicking holograms, lenses or diffraction gratings, aiming at creating unique field structures that are not attainable with conventional optical elements. Below, we will consider two examples of such metasurfaces.

We envisage that an important direction for metasurfaces is the generation of superoscillatory fields. Indeed, a conventional lens cannot focus free-space light beyond half of the wavelength, λ. Nevertheless, precisely tailored interference of multiple waves can form a hotspot in free space of arbitrarily small size known as superoscillation.

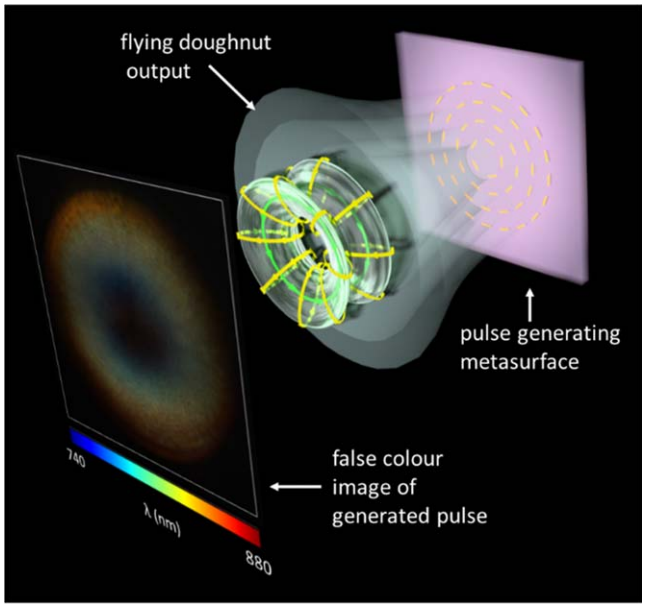

Figure 6. Sketch of metamaterial converter for the generation of flying doughnut pulses. The metasurface consists of azimuthally oriented dipole resonators arranged in concentric rings. The inset at the bottom left of the figure shows a false colour image of a flying doughnut pulse, experimentally generated by a plasmonic metasurface (fabricated by focused-ion-beam milling) [53]. The high frequency components close to the centre of the pulse are indicated by the blue-green colour, while the red colour in the periphery of the pulse corresponds to the lower frequency components, in accordance with the space-time non-separable nature of the pulse.

Recently, a new type of metasurface was demonstrated that generated electromagnetic field profiles with structural features at the $\lambda/100$ scale in free space [50]. The metasurface creates a sub-diffraction hotspot surrounded by nanoscale phase singularities ($\sim\lambda/50$ in size) and zones where the phase of the wave changes more than tenfold faster than in a standing wave. These areas with high local wavevectors are pinned to phase vortices and zones of energy backflow ($\sim\lambda/20$ in size) that contribute to subtle and relatively small tightening of the main focal spot size beyond the Abbe-Rayleigh limit. Such superoscillatory free space fields offer new opportunities for nanoscale metrology and imaging.

Another direction of research where metasurfaces can be indispensable is the generation of non-separable space-time electromagnetic excitations that exist only in the form of short bursts of energy propagating in free space at the speed of light. Typical examples of such excitations are the 'flying doughnuts' [51], which are distinguished from transverse waves by a doughnut-like configuration of electric and magnetic fields with strong longitudinal field components along the propagation direction.

The generation of flying doughnut pulses presents a number of substantial challenges associated to their unusual spatiotemporal structure. For example, the few-cycle nature of the pulse requires a broadband source, while the frequency

content of the pulse varies substantially along the radial direction. Such flying doughnuts can be generated from conventional pulses using a singular metamaterial converter designed to manipulate both the spatial and spectral structure of an input pulse [52, 53]. The metamaterial converter can be constructed by a cylindrically symmetric array of low Q-factor dipole resonators oriented radially or azimuthally oriented electric dipoles and arranged in concentric rings (see figure 6). The spatiotemporal coupling is provided by varying the resonant properties of the metamaterial elements across the radial direction. The ability to generate flying doughnuts is of fundamental interest, and as such pulses shall interact with matter in unique ways, including nontrivial field transformations upon reflection from interfaces and the excitation of toroidal response and anapole modes in matter, hence offering opportunities for telecommunications, sensing, and spectroscopy.

Acknowledgments

This work was supported by the Singapore Ministry of Education (Tier 3 Grant MOE2016), the Engineering and Physical Sciences Research Council UK (Grant EP/M009122/1), and the European Research Council (ERC) under the European Union's Horizon 2020 research and innovation programme (Grant Agreement No. 786851).

5. Refractory plasmonic metasurfaces

Sajid Choudhury, Zhaxylyk A Kudyshev, Soham Saha, Harsha Reddy, Alexandra Boltasseva, Vladimir M Shalaev and Alexander V Kildishev

School of Electrical & Computer Engineering and Birck Nanotechnology Center, Purdue University, West Lafayette, IN 47907, United States of America

Status. Optical metasurfaces (MSs) emerged with the promise of manipulating light at a sub-wavelength scale. The concept of MSs has been utilized to create ultra-compact and subwavelength flat optical elements—lenses, holograms, color filters, waveplates, etc. (For more detailed reviews on MS applications, please refer to [54–66]). However, plasmonic and dielectric MSs have been broadly used primarily for room temperature applications. The inherently small footprint for MS components requires a tradeoff between the high field confinement and lower damage threshold. In dielectric MSs, the losses are lower and thus this class of MSs could be used to make high-temperature devices. However, the field confinement in a dielectric MS is much smaller than in its plasmonic counterparts. Additionally, losses are beneficial in applications where the power absorbed through loss is harvested as heat.

Thermal to photovoltaic energy conversion can be obtained by selectively converting heat energy to emitted radiation at a wavelength. The radiation is then absorbed by a photovoltaic (PV) cell that converts it to an electromotive force to drive external current through a circuit. A solar absorber can be combined with the emitter to convert solar energy first to heat and then to the selective radiation band corresponding to the PV cell. Recently, it has been theoretically predicted that by judiciously tailoring the spectral properties of the emitters and absorbers components using metasurfaces, the efficiency for direct energy conversion from solar/thermal energy to electricity could potentially reach an unprecedented value of ∼85% [67]. This estimated theoretical efficiency is in striking contrast to the current physical limitation (∼30%) imposed by the Shockley-Queisser limit [68] for a single silicon p-n junction cell [69]. The development of optical MS structures would open new frontiers for realization of solar thermophotovoltaic and thermophotovoltaic systems. Both systems require metasurface elements operating at a very high temperature (>1000 °C).

Thermophotovoltaics (TPV). In a TPV system, thermal radiation is directly converted to electricity via the photovoltaic (PV) effect. A TPV system consists of a PV cell array and a selective emitter with the emissivity matching absorption band of a PV cell. A schematic of a TPV system is shown in figure 7(a). TPV energy conversion offers numerous significant advantages over competing technologies [70, 71]. These include the realization of highly versatile, modular, low-weight and compact electric generators (portable or stationary), which are noiseless, low-maintenance and energy-efficient [72]. Optimal TPV energy conversion requires large area metasurface emitters (see figure 7(a)). Hence, robust refractory materials, which are compatible with low-cost, large-area fabrication-techniques, are critical for practical highly-efficient metasurface TPV elements.

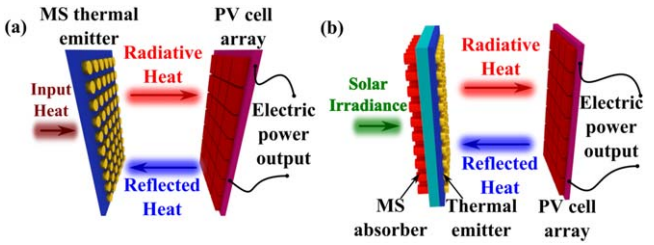

Figure 7. Schematics of TPV (a) and STPV (b) systems. Metasurface emitters are heated with the heat source (TPV) or with solar irradiance in STPV using broadband absorbers and the emission is used to power PV cells.

Solar thermophotovoltaics (STPV). An STPV system comprises an absorber, an emitter, and PV cells, as shown in figure 7(b). The absorber, heated by concentrated solar energy, increases the temperature of the emitter, which is engineered to radiate within the specific band where the absorption of a PV cell is at its maximum. Hence, by absorbing broadband solar energy and then re-emitting it within a desired working band of the PV cell array, the MS-based STPV architecture provides an efficient way of harvesting solar energy [69].

Current and future challenges. The inherent ability of MSs to tailor the absorbances/emittances of optical surfaces is of great interest in TPV and STPV. The functionality of MSs can be further enhanced by designing emitters that operate at elevated temperatures and match the spectrum of solar radiation, thus maximizing the absorption. MS resonant superabsorbers have already demonstrated polarization independent absorption in the entire visible spectrum [73]. The absorption/emission can also be engineered to match that of energies emitted by other forms of radiative emitters, such as a nuclear reactor, engine, or combustion chamber [74]. Plasmonic metasurface emitters for STPV and TPV require materials that maintain good optical properties at high-temperatures and field intensities [75]. Conventional noble metals (Au and Ag) have low melting points and damage thresholds. Nano-structuring these materials further decreases the maximum temperature that they can withstand. At high temperatures, gold MSs were shown to deform [76]. Passivation with a dielectric was shown to improve the performance of gold MSs at high field intensities [77]. While TiN is CMOS compatible, many of the processes used to grow TiN involve the use of lattice matched substrates and high temperatures, which limits its practical applicability. The material also oxidizes at elevated temperatures, which makes it important to passivate with a suitable capping layer [77]. Yet, there have been few investigations on the high-temperature properties of thermally stable dielectric capping layers. As refractory plasmonic materials are inherently

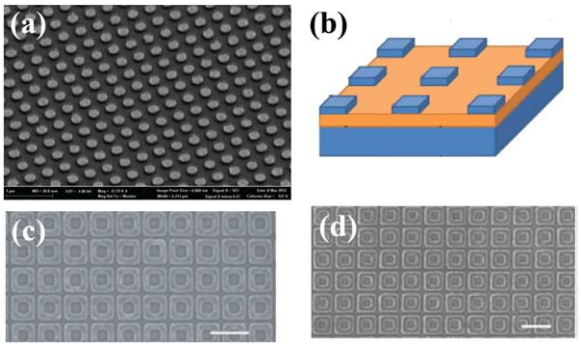

Figure 8. Various refractory metasurface devices. (a) Pt based high T emitters [79]**.** (b) TPV emitter with tungsten [80]. (c), (d) TiN based broadband absorber with (c) 800 °C annealing and (d) 6.67 W cm^{-2} laser illumination [76]. (a) Reprinted from [79], with the permission of AIP Publishing (2014). (b) Reprinted from [80], Copyright 2013, with permission from Elsevier. (c), (d) [76] John Wiley & Sons © 2014 WILEY-VCH Verlag GmbH & Co. KGaA, Weinheim.

robust, they often require special growth conditions to reduce optical losses and require sophisticated etch chemistry to pattern them. A new material platform would also require the characterization of high-temperature optical properties to design the MS structures for different applications. The optical properties of a material are heavily dependent on different growth conditions and crystal properties [78], which necessitates further optimization for the best plasmonic response. Material research is needed to explore possible refractory materials that would have comparable optical properties to Ag and Al. Also, for any new material platform, there is the challenge of developing a scalable patterning recipe.

Solutions to the problem

Conventional refractory materials. With the advent of new material research, alternatives to noble metals were explored for plasmonics. The first choices for replacing them were high melting point metals, such as platinum (Pt) and tungsten (W). The lower real-part of the permittivity and the higher losses of refractory materials compared to noble metals are usually compensated with gap-plasmon structures. Pt was explored as a candidate for TPV emitters, with a Pt disk resonator and an alumina spacer which can withstand heating cycles of up to 650 °C [79]. Figure 8(a) shows a SEM image of the disks. High-temperature applications with W were also explored for TPV. Gap-plasmon structure with a SiO_2 spacer (see figure 8(b) [80]) and W gratings with a SiO_2 protective film [81] showed suitable emission properties from 400 nm to 2000 nm wavelength range.

Refractory transition metal nitrides. Titanium and zirconium nitrides (TiN and ZrN) are promising alternatives to these high loss materials and demonstrate superior optical functionality at high temperatures. Though they exhibit higher losses compared to Au or Al, they can withstand significantly higher temperatures [82]. A broadband absorber has been demonstrated using a bilayer TiN/SiO2 and patterning the top TiN into square-shaped loop shapes. The structure has shown a higher damage threshold and stability to annealing compared to a similar structure made with gold [76]. Figure 8(c) shows the TiN MS after annealing at 800 °C, and figure 8(d) shows the same TiN structure surviving laser illumination at 6.67 W cm^{-2}, proving a higher damage threshold in comparison to Au. Moreover, recent studies indicate that temperature-dependent optical properties of epitaxial TiN degrade at a much lower rate with increasing temperature compared to Au or Ag [83]. Also, fabricated epitaxial TiN-based nanodisk arrays show a broader optical absorption and a better tolerance to diameter variation [84]. Multi-objective optimization of TiN nanohole MSs, generating arbitrary far-field optical patterns, has been demonstrated using an evolutionary algorithm [85]. Refractory ZrN has been patterned to prepare a photonic-spin-Hall-effect (PSHE)-based MS for spectroscopic application [86].

Passivating refractory layers. Noble metals have already been reported to be used in absorbers with protective capping layers that enhance their stability. With a 4-nm passivating alumina layer, noble metals can withstand a temperature of up to 800 °C [77]. With annealed deformation of a gold film, gold islands were formed on alumina and indium doped tin oxide (ITO) and the resulting structure has been used to make emitters at 900 °C with 22-hour long exposures in an oxidizing environment [87]. Alumina-passivated Pt disks can be heated up to 1055 °C and have reported a power conversion efficiency of 24% [88]. With these results, the use of passivating refractory nitrides with matching refractory ceramics shows further promise of increasing the damage threshold and robustness of the structures [89].

Near-term goals. In addition to the technological advancements mentioned above, the following challenges need to be overcome for a MS based on a refractory material to be commercially viable. First, TiN needs to be grown at a low temperature while maintaining good plasmonic properties. Second, new etch recipes need to be developed which can etch refractory materials while retaining the optical properties. Then, CMOS compatible, low loss, dielectric materials should be developed to survive high temperatures and should be compatible with a refractory material platform. Finally, new materials should be explored at elevated temperatures for refractory plasmonic applications.

Concluding remarks. Refractory plasmonic MSs are establishing a field for potential markets where not only high temperatures but harsh environments in general need to be tolerated. The applications could go beyond solar and waste heat harvesting and include high temperature and high-power sensors, heat-assisted magnetic recording (HAMR), and photocatalysis—the areas that could potentially benefit from the use of refractory MS optical elements. Unparalleled functional benefits could be offered by refractory metasurfaces equipped with novel plasmonic materials. Their implementation in practical systems and mass production are the next milestones to be achieved.

Acknowledgments

The authors acknowledge the Air Force Office of Scientific Research Grants FA9550-14-1-0389, FA9550-18-1-0002 and DARPA/DSO Extreme Optics and Imaging (EXTREME) Program, Award HR00111720032. The authors acknowledge D Shah for assistance with preparing the manuscript.

RECONFIGURABLE AND ACTIVE METASURFACES

6. Current and future directions in tunable and active metasurfaces

Daniel Sievenpiper

University of California, San Diego, CA, United States of America

Status. The field of tunable and active metasurfaces includes a wide variety of structures and a range of applications, but they share several common features. They typically involve periodically patterned metal structures, which are commonly made using printed circuit boards for radio frequency applications but can also be constructed of other materials for THz or optical frequencies. In order to reconfigure their electromagnetic properties, they require tunable devices or materials in each unit cell. The variation in effective material properties can often be described as a tunable surface impedance, although more complex descriptions are required when nonlinearity is included. As an example, metasurfaces for electronic beam steering can incorporate varactor diodes to control the capacitance between neighboring cells, thereby manipulating the surface impedance and corresponding reflection phase [90]. Similar behavior can also be achieved with liquid crystals. Other kinds of active surfaces may involve nonlinear switchable behavior that responds to the incoming power level, various forms of feedback control, or active electronics for increasing bandwidth.

The control signal for reconfiguring the surface can either be applied explicitly through a series of control wires, which greatly increases the complexity, or for some applications they can be applied indirectly through the incoming RF wave itself. Examples of the latter type include the subfield of nonlinear surfaces, which change their properties in response to the incoming signals. This may involve simple diodes which can reconfigure the surface from a low loss state to a highly absorbing state as the RF power increases [91]. Transistors can be used in the place of diodes to provide a sharper response curve, in order to allow for the use of feedback to enable control over the turn-on threshold power [92]. Each of these surfaces can be switched between low-loss and high-loss states to mitigate the damaging effects of high-power signals, or to control the gain of nearby antennas.

Nonlinear surfaces can also enable properties that are not possible with linear or passive materials. For example, using a slightly more complex diode bridge circuit it is possible to create a waveform selective absorber for surface waves. In contrast to conventional absorbers, which are generally frequency-dependent, these materials can selectively respond to different waveforms, such as long or short pulses, even within the same frequency band, as shown in figure 9 [93]. By combining feedback control with varactor tuning of the surface absorption band, it is also possible to create a surface that automatically tunes its maximum absorption frequency to match the incoming signal [94]. Although such surfaces have narrow instantaneous bandwidth, they can be broadly tunable, exceeding the fundamental limits of passive absorbers [95]. In other examples of the use of feedback in metasurfaces, varactor-controlled surface impedance can enable self-focusing of microwaves [96], analogous to the optical phenomenon of the same name.

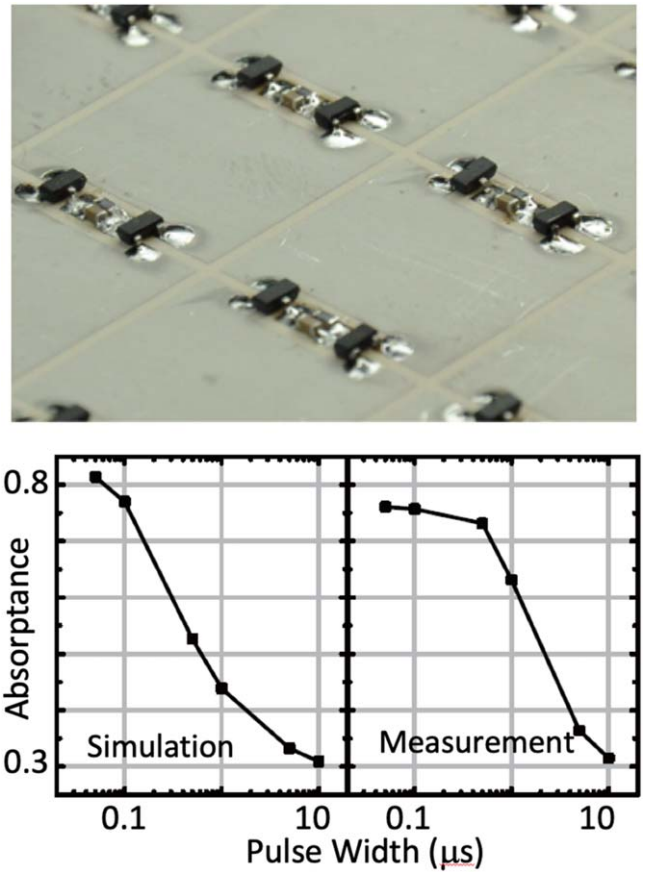

Figure 9. First waveform-dependent absorber which uses a diode bridge and RC circuit to selectively respond to the envelope of the incoming signal rather than simply its frequency.

In addition to those employing simple feedback control, other types of active metasurfaces have also been developed. For example, non-Foster circuits [97] use cross-coupled transistors to achieve an effective negative capacitance or negative inductance. This can be used to significantly extend the bandwidth of active metasurfaces beyond the fundamental limits that govern completely passive structures. In a typical design, one simulates the structure with various reactance values to achieve a particular goal, such as a constant surface impedance over a given frequency band. The required reactance may have a negative slope with frequency, indicating that a non-Foster element is required. Using this approach, artificial impedance surfaces have been built with nearly an octave of bandwidth in the UHF range with a thickness of only 5 mm, far thinner than the fundamental limit for passive surfaces [98]. An example of such a structure is shown in figure 10.

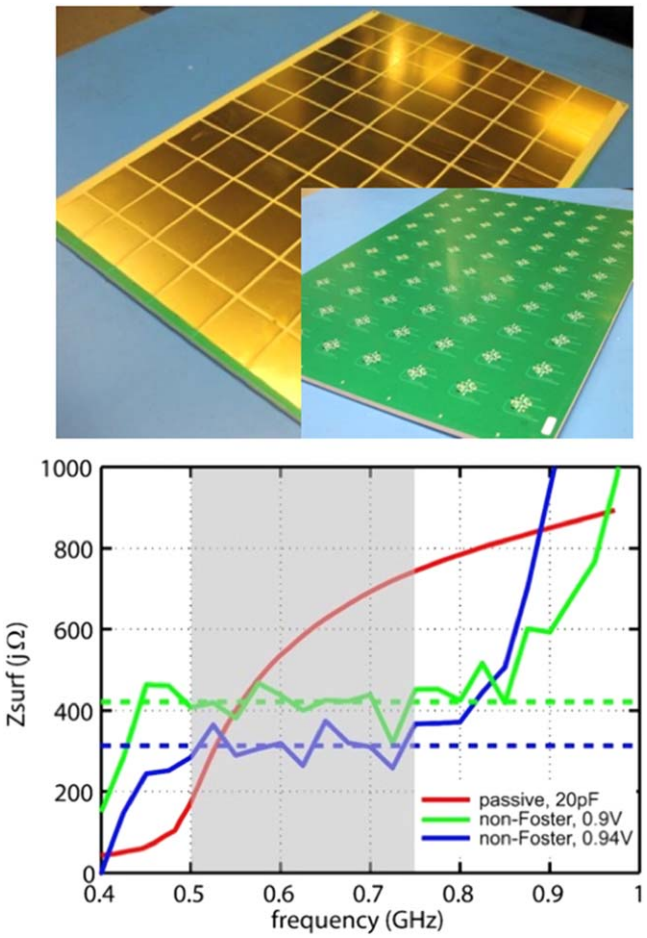

Figure 10. Active impedance surface with metal patches on front and non-Foster circuits on back, and measured data indicating roughly 300j Ω impedance over nearly an octave of bandwidth, with a thickness of 5 mm. © 2016 IEEE. Reprinted, with permission, from [98].

At optical frequencies, active surfaces may involve the combination of optical and electrical excitation, such as to excite a plasma, or induce photoemission [99]. These can enable a wide variety of new optical and electronic devices including metasurface-based all-metal photodetectors and optical rectifiers, as well as new kinds of vacuum transistors [100]. In the optical range, the combination of plasmonic effects with field enhancement through the use of metasurfaces is particularly exciting.

Current and future challenges. One of the biggest limitations in existing tunable and active metasurfaces involves the breakdown or nonlinearity that can occur under high-power illumination when the surface contains semiconductor components such as varactors or transistors. This can limit the power handling capability of self-tuning absorbers, self-focusing structures, and other kinds of active surfaces. Because one application for nonlinear metasurfaces is mitigation of high-power microwave signals, this represents a significant limitation. For beam steering applications, nonlinearities can result in the generation of unwanted harmonics, as well as artifacts in the radiation pattern due to the tendency to self-steer under high power. Other tuning mechanisms also exist, such as liquid crystals [101], or other ferroelectrics [102], but they have their own limitations including temperature effects or high voltage requirements.

A more fundamental limitation relates to the bandwidth, thickness, and absorption capabilities of absorbing metasurfaces. Self-tuning structures can achieve broader tuning bandwidth without sacrificing the other performance parameters, but an absorber that exceeds the fundamental limit with broad instantaneous bandwidth is still elusive. Additional practical limitations include the significant complexity required to address and drive a large number of tuning devices on the surface. It is also currently impractical to reach the upper mmW band due to inherent parasitic effects in semiconductor devices. Lithographic limits often impose restrictions on the kinds of optical devices that can be built, and the THz band remains a difficult frequency range to achieve for most technologies.

Tuning elements such as varactors also introduce their own losses. As a general rule, those losses will be significant if the quality factor of the tuning device (defined by the ratio of its resistance to its reactance) is not significantly larger than the intrinsic quality factor of the metasurface (defined by the inverse of its instantaneous bandwidth). This indicates that thicker surfaces with broader bandwidths will have lower loss, but this must be balanced with practical thickness limitations, as well as considerations of the limited utility of a metasurface that has a narrower tuning range than its own instantaneous bandwidth.

Advances in science and technology to meet challenges. New advances in technology can mitigate some of the limitations described above. For example, the use of plasma devices or emerging vacuum electronic devices for high power applications such as absorbers can avoid damage due to breakdown, as well as nonlinear effects. For beam steering applications, mechanical varactors such as MEMS devices [103] are available and can also minimize nonlinearities because the mechanical parts do not respond at the frequency of the RF signals. Development of advanced liquid crystals or ferroelectric materials may have similar benefits.

Newly developed nonreciprocal devices involving switching or modulation may be incorporated into future metasurfaces to provide a way to exceed the fundamental bandwidth limitations that plague existing tunable absorbers. Similar behavior can also be obtained by incorporating conventional nonreciprocal magnetic materials such as those involving the Faraday effect. Finally, new emerging types of materials such as topological photonic insulators and the related chiral materials may provide new physics for capabilities beyond those described here. For example, such structures may provide one-way surface wave propagation, or enable one-way radomes for RF signals.

Concluding remarks. Tunable or active metasurfaces provide a way to do what is not possible with passive materials, such as

circumventing the fundamental limits of absorbers, achieving high isolation among nearby devices or preventing damage from high power signals. They also provide ways to create electronically steerable antennas, or to manipulate surface impedance. Currently, they are limited by the devices that are used for tuning, or by the same fundamental limitations of passive materials, such as the thickness/bandwidth tradeoff. New devices under development such as plasma or vacuum electronics may provide a solution to power limitations, while new concepts in active and nonreciprocal devices and other related structures and may enable advancements beyond the limits of passive materials or the emergence of new capabilities.

Acknowledgments

This work has been supported by AFOSR through grant FA9550-16-1-0093, by ONR through Grant N00014-15-1-2062, by NSF through Grant 1306055, and by DARPA through contract N00014-13-1-0618 and W911NF-17-1-0580.

7. Nonreciprocal metasurfaces

Christophe Caloz

Polytechnique Montréal, Canada

Status. Nonreciprocity is the property of a transmission system—specifically, a medium or a component—exhibiting different received-to-emitted field ratios between specified ports (terminals with specific mode, polarization and frequency)[22] when the source and detection roles of these ports are exchanged [104]. It is equivalent to time reversal (TR) symmetry breaking, or TR asymmetry [105], in the limit of vanishingly small loss and radiation. However, lossy and radiative systems are TR-asymmetric even when reciprocal; they are symmetric only in terms of field ratios [104], consistently with the above definition. Therefore, TR asymmetry is not a sufficient condition but only a necessary condition for nonreciprocity.

The history of nonreciprocal science and technology spans more than 170 years [104]. It started with the experimental discovery by Faraday of the eponymic rotation effect near 1845 [106], which led to the exploration of the first nonreciprocal structures in the second part of the 19th century. A next milestone was the theoretical derivation by Onsager of reciprocity relations for macroscopically irreversible processes in the 1930s [107]. The five decades following World War II witnessed a massive development of ferrite-based nonreciprocal components—particularly isolators, circulators, gyrators and nonreciprocal phase shifters—that are now ubiquitous in microwave and optical technologies. Finally, the crystallographic incompatibility of ferrites with integrated circuits spurred an ardent quest for magnetless nonreciprocal systems at the turn of the 21st century [108].

While most conventional nonreciprocal systems are 1D waveguide-type components, extending the realm of such systems to higher dimensions will likely bring a cornucopia of novel physical effects and industrial applications. Metasurfaces, given their combined simple 2D topology and unprecedented capability to transform 3D waves, represent an ideal platform for such developments. Figure 11 shows straightforward applications of nonreciprocal metasurfaces. Early contributions in this field include the works reported in [109–118], which will be discussed in the next section.

Current and future challenges. Figure 12(a) represents a generic nonreciprocal metasurface structure and operation. It differs from reciprocal metasurfaces essentially by the extra presence of TR-breaking mechanism that will be described shortly. Nonreciprocal metasurfaces—as all nonreciprocal systems—may be classified as linear or nonlinear, with the former category further dividing into linear time-invariant (LTI) and linear time-variant (LTV) structures [104]. They present great potential, but also pose considerable challenges.

[22] The specification of ports is crucial for the qualification of reciprocity or nonreciprocity. Many asymmetric systems have distinct field distributions in different propagation directions across the systems while having identical port-to-port ratios, thereby fallaciously appearing nonreciprocal [104].

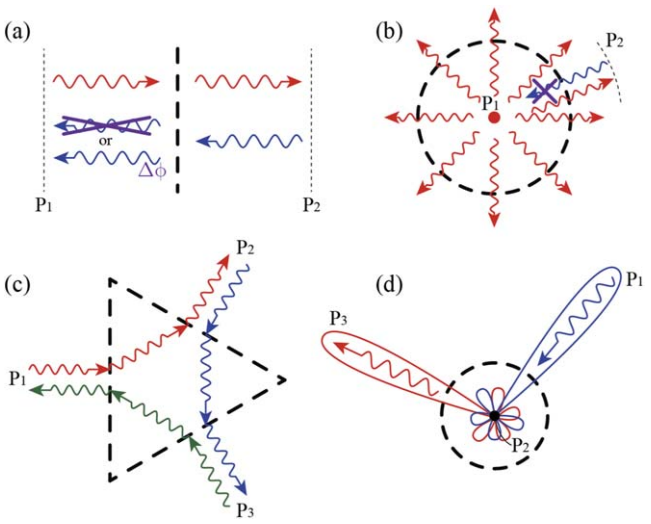

Figure 11. Conceptual representation of typical applications of nonreciprocal metasurfaces (thick dashed curves) with port n labelled P_n. (a) Planar spatial isolator or nonreciprocal phase shifter. (b) Spherical isolator. (c) Spatial circulator. (d) Transmit-receive radiation pattern discriminator.

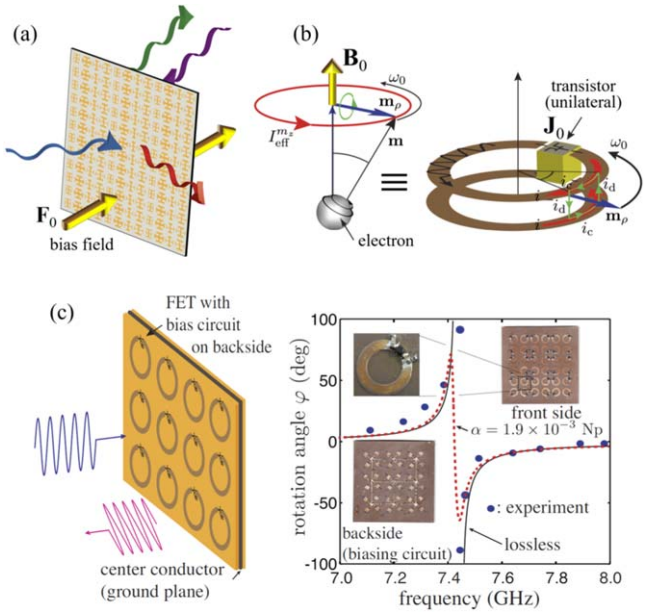

Figure 12. (a) Generic representation of a nonreciprocal metasurface, with bias field $\mathbf{F}_0$. (b) Magnetless transistor-loaded ring metamaterial particle, mimicking electron spin precession in ferrites, with current $\mathbf{J}_0$ operating as the biasing field [110–112]. (c) Reflective Faraday ring metasurface based on the particle in (b). (Left) Perspective view of the metasurface structure. (Right) Faraday rotation angle versus frequency obtained theoretically from the equivalent magnetic Polder tensor (dashed and solid curves) and experimentally from the prototype shown in the insets (dots) [110].

We shall only discuss linear nonreciprocal metasurfaces here, whose TR symmetry is broken by a time-odd external field $\mathbf{F}_0$ [105], called the biasing field, and leave out their nonlinear counterparts because of their prohibitive limitations, in terms of intensity dependence, one-way-at-time-only operation, and weak nonreciprocity or hysteresis [104].

In LTI nonreciprocal metasurfaces, the biasing field is static. An LTI spatial isolator (figure 11(a)) can be realized, in both the microwave and optical regimes, by placing a ferrite slab, biased by a magnetic field $\mathbf{F}_0 = \mathbf{B}_0$, between mutually $\pi/4$-rotated conductive-resistive grid pairs [109]. However, such a device is of limited practicality because the required biasing either limits it to local operation (electromagnet poles sandwiching the overall system along the propagation axis) or implies excessive complexity (powerful coil coaxially wounded around the system).

A more propitious LTI nonreciprocity technology is that of metasurfaces based on transistor-loaded ring particles, whose biasing field is the current feeding the transistors $\mathbf{F}_0 = \mathbf{J}_0$ [110]. Figure 12(a) depicts such a metasurface, which mimics electron spin precession in real ferrites, leading to a quasi-perfect 'artificial ferrite,' with identical Polder tensorial description and electromagnetic properties—including Faraday rotation[23]. Such metasurfaces/metamaterials have already been demonstrated in various nonreciprocal components [111] and antenna systems [112]. They represent a unique magnetless alternative to ferrite technology, not only resolving the ferrite issue of integration, but also allowing flexible operation frequency, multi-resonances (using concentric rings of different diameters) and hence multi-band devices, and electronic Faraday rotation direction flipping (using antiparallel transistor pairs).

Transistors are unfortunately not available in the optical regime. However, the function of transistors in LTI metasurfaces may be replaced by the injection of a time-varying perturbation, called modulation, for application to the optical regime. In this case, the metasurface becomes LTV, because the modulation induces time-varying effective medium parameters [114]. Ipso facto, the modulation plays the role of the biasing field, characterized by the modulation velocity (time-odd quantity) $\mathbf{F}_0 = \mathbf{V}_0$, and is hence dynamic. LTV may also lead to a great diversity of metasurface systems. However, no LTV nonreciprocal metasurface has been experimentally demonstrated yet to date.

The nonreciprocal metasurfaces in [110] (or figures 12(b) and (c)) have been experimentally demonstrated only as Faraday rotators, although transistor-loaded ring particles were also applied to several guided-wave components [111] and antennas [112]. However, once realized in the transmission—rather than reflection—mode, they will readily enable spatial isolators (figure 11(a)) using a rotated grid configuration [109], spatial gyrators and nonreciprocal phase shifters (figure 11(a)) ensuring 180° Faraday rotation and phase control via transistor design, and possibly spherical radomes with some technical feats. If Faraday rotation is not required, or even undesired (e.g. need for unaltered polarization state), then a simple nongyrotropic metasurface isolator can be realized using the array-circuit-array philosophy in [113], as reported in [115]; such a metasurface may find applications in instrumentation, sensing and communications. More sophisticated metasurface systems, having some similarities with the circulator in figure 11(c), have been conceptually described in [116–118], but these systems have not been experimentally realized yet. Finally, a nonreciprocal radiation pattern system (figure 11(d)) based on a nonreciprocal and dispersion-engineered antenna feeding network has been reported in [119], but the related metasurface realization is still missing.

Advances in science and technology to meet these challenges. The major challenge in nonreciprocal metasurfaces resides in their practical implementation. Problems to be solved in this regard include: (1) the elaboration of efficient strategies for decoupling the biasing network from the electromagnetic structure, using for instance field-orthogonal thin strips; (2) the extension of existing LTI concepts to the terahertz regime, using latest integrated circuit technologies; (3) the boosting of power handling, resorting to semiconductors such as InP/GaN and to LDMOS transistor architectures; (4) the conception of (statically-biased) LTI structures in the optical regime, so as to avoid the LTV difficulties of modulation injection and source complexity; and (5) the development of efficient microwave, terahertz and optical chips for industrial deployment. LTV metasurfaces are particularly challenging, but also represent novel opportunities for engineering the temporal spectrum, in addition to the spatial spectrum, of electromagnetic waves and light.

Concluding remarks. Nonreciprocity dramatically enriches the palette of metasurface properties, and nonreciprocal metasurfaces, despite substantial technical challenges, represent a most promising emerging field of science and technology. In the near future, they will likely open new horizons for a diversity of applications, such as the control of thermal radiation for energy saving, the molding of radiation pressure forces for the manipulation of nanoparticles, and the design of key devices in quantum photonics and computing.

[23] An alternative for a Faraday metasurface was reported in [113] in the form of a pair of back-to-back twisted dipole antenna arrays interconnected by transistors. However, this structure is more akin to a circuit system than a metamaterial and does not include the fundamental properties of ferrites.

8. Active and reconfigurable metasurfaces

Andrea Alu`

Photonics Initiative, Advanced Science Research Center, City University of New York, New York, United States of America

Status. Metasurfaces have opened up exciting opportunities in electromagnetic and photonic research in the past decade, as outlined in this Roadmap. The original proposals in this field suffered from inherently limited efficiencies and sub-optimal designs, but steady advances in the theoretical understanding of wave interactions with metasurfaces and in the associated fabrication processes have shown that a single, ultrathin patterned surface can provide unprecedented opportunities to tailor the impinging wavefront with large efficiency, within a practically viable technology. As the fields mature, it has become clear that, in addition to efficiency and extreme wavefront manipulation, an important feature required in many applications is agile tunability and reconfigurability. While most realizations of metasurfaces to date have been strictly passive and static, recent efforts have indeed explored opportunities to include active elements in the metasurface unit cells at microwave, infrared and optical frequencies [120–124], opening exciting opportunities to broaden the impact of this technology for various practical goals and applications. Active elements not only provide ways to reconfigure the response in real time, but also to compensate loss and overcome fundamental challenges of passive metasurface technology.

Current and future challenges. Reconfigurable and active metasurfaces hold the promise to drastically advance this field of technology and to overcome its current limitations, yet these features come with several challenges to be confronted. At microwave and mm-wave frequencies, some form of tunability is relatively simple to achieve using variable capacitors, switches, or other lumped elements that can be modulated in time. These elements have been explored in several metasurface implementations, e.g. [121, 124], showing that it is indeed possible to reconfigure in real time the response of the surface with sufficient freedom. Figure 13 shows an example of a reconfigurable Huygens metasurface realized loading split-ring resonators with variable capacitors, yielding efficient manipulation of the impinging wavefront and some form of reconfigurability.

However, the speed and depth of modulation offered by these solutions are often limited, and there is a trade-off between these metrics and the power handling that these elements can offer. Advances in modulation technology are required to meet the demands of wireless and radar applications, and to broaden their scope to more sophisticated wave transformations exploiting fast temporal modulations [125]. In this context, the use of active and non-Foster lumped elements becomes of great interest to also overcome the inherent bandwidth limitations of passive metasurfaces [124] and improve their overall efficiency.

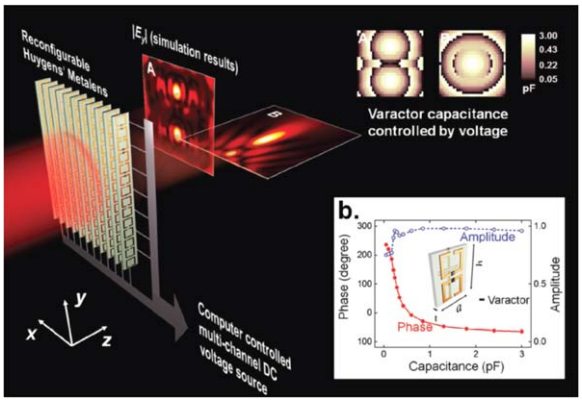

Figure 13. Reconfigurable metasurface realized with split-ring resonators loaded by tunable lumped elements. [121] John Wiley & Sons. © 2017 WILEY-VCH Verlag GmbH & Co. KGaA, Weinheim.

As the frequency of operation increases, reconfigurability and tunability become even more challenging. Electrooptical modulation has been explored in graphene-based metasurfaces to provide some basic form of reconfigurability [120]. Electromechanical [122], optomechanical, acoustoelectric and other multiphysics phenomena may also be exploited to modulate in time the metasurface elements and enable reconfigurability. Phase-change materials are another recent material platform that hold great promise to enable a moderately fast reconfigurable response [123]. However, these solutions all suffer from some form of tradeoff, with modulation speed and depth again being the limiting factors in achieving reconfigurability and efficiency at the same time, and inherent bandwidth and loss constraints.

The integration of gain to realize active metasurfaces is also at its infancy in photonics, given the challenges to provide the required level of gain at high frequencies. We should also mention the inherent challenges with stability that need to be considered when dealing with active elements in arrays, especially when dealing with applications requiring broadband and extreme forms of wave manipulation [127].

Recent advances in the science and technology of active and reconfigurable metasurfaces. While it is clear that several challenges need to be faced and overcome to bring active and reconfigurable metasurface technology to mainstream use, it is also evident that the benefits of these advances would be important. Reconfigurable ultrathin surfaces that provide real-time extreme wavefront transformations to the impinging photons would have a significant impact in nearly any electromagnetic and photonic application, from classical to quantum photonics, from radar to wireless technology.

As the available modulation speeds and depths improve with progress in materials and fabrication techniques, unprecedented opportunities arise for metasurface technology. For instance, as the modulation frequency becomes comparable to the bandwidth of operation of the metasurface, highly unusual wavefront manipulation schemes become available, beyond what is achievable in passive, time-invariant systems. Non-reciprocal scattering responses can

be supported by space-time varying metasurfaces, yielding one-way ultrathin mirrors that reflect when excited from one direction, but transmit in the opposite direction [125], as outlined in the previous section. In addition, energy exchanges between modulation and impinging signals become possible at sufficiently high speeds, opening a path towards noise-free active metasurfaces.

Active metasurface responses are of special interest in various realms of technology. First, active metasurfaces can overcome the inherent limitations of passive, linear, time-invariant devices. As an example, figures 14(a)–(c) show a metasurface cloak, composed of an array of subwavelength metallic patches, loaded at the gaps with active lumped elements. Their frequency dispersion violates Foster's reactance theorem, which forces any passive element with low loss to have a growing reactance with frequency. The effective surface reactance of this metasurface therefore decreases with frequency. When coupled to the growing reactance of a passive object, the overall response can be tailored to offer low scattering over a wide bandwidth, yielding a large increase in the bandwidth of operation of metasurfaces for radar scattering suppression [124]. Similar concepts may be applied to other application areas, in order to broaden the bandwidth of metasurfaces beyond the limitations imposed by passivity, and to compensate loss.

Gain and active metasurfaces are also exciting in the context of the recent research activity on parity-time (PT) symmetry. Originally introduced in quantum mechanics, this special symmetry requires a strict balance between loss and gain, so that the system as a whole is symmetric upon a concurrent inversion in space and time. This symmetry condition has opened up interesting opportunities in optics and photonics in recent years [126], including unusual scattering and lasing properties. Active metasurfaces offer an ideal playground to realize these phenomena [127–129] in compact and flexible geometries, with a variety of opportunities to manipulate light. As an example, figure 14(d) shows a PT-symmetric pair of metasurfaces, one passive and one active, which, when placed in front of each other, support all-angle negative refraction without reflections. These unusual features have been proposed to realize flat lenses that can focus images without aberration, as shown in figure 14(d) [127], as well as efficient sensors that do not leave shadows [128]. PT-symmetric metasurfaces can also realize electromagnetic cloaks that do not obey the strict trade-off between size and bandwidth of passive systems [129]. More broadly, PT-symmetric metasurfaces offer an elegant way to establish automatic feedback, ensuring the stable response of interest as the background changes in time. Realizing these concepts, especially at visible frequencies, requires large levels of gain, unavailable with current technology, but opportunities offered by time modulation or multi-physics phenomena, such as optomechanical coupling, may offer a viable opportunity forward to integrate gain in metasurfaces.

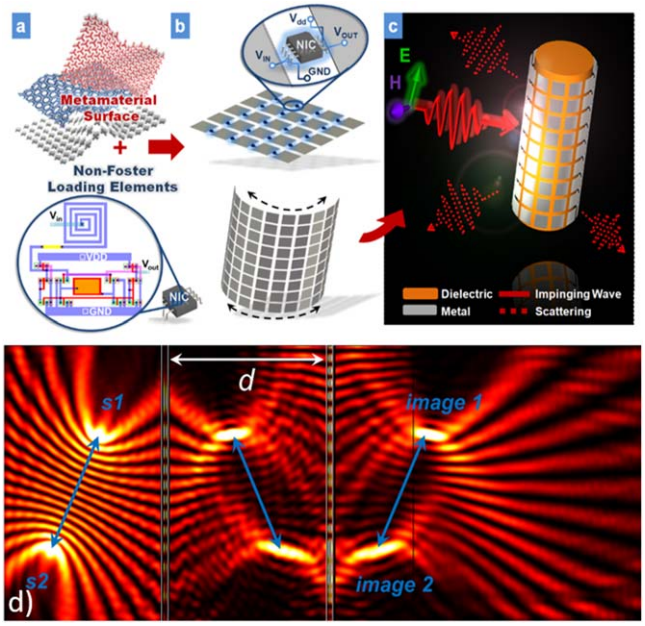

Figure 14. Active metasurfaces to broaden the bandwidth and enable parity-time symmetric operation. (a)–(c) Non-Foster metasurfaces, loaded with active lumped elements, for broadband cloaking technology [124]. (d) Parity-time symmetric metasurface for flat, aberration-free imaging [127]. (a)–(c) Reprinted figure with permission from [124], Copyright (2013) by the American Physical Society. (d) Reprinted figure with permission from [127], Copyright (2016) by the American Physical Society. CC BY 3.0.

Concluding remarks. As the field of metasurfaces matures, it is clear that reconfigurability and active unit cells become of primary importance to make this technology practically viable and of broad impact from radio-frequencies to optics and photonics. Despite various technological challenges, the steady progress in theoretical concepts, material science, modulation schemes, and nanofabrication techniques, offers a rosy prospective on the future of active and reconfigurable metasurfaces. We envision metasurfaces with integrated feedback that respond in real-time to changes in the environment for the next generation of sensing, storing, computing and imaging devices based on light.

Acknowledgments

I would like to thank my past and present group members and collaborators for their work on the topic of active and reconfigurable metasurfaces, and the support of the US Department of Defense, the National Science Foundation, and the Simons Foundation.

9. Tunable metasurfaces

Qiong He and Lei Zhou

State Key Laboratory of Surface Physics and Physics Department, Fudan University, Shanghai 200433, People's Republic of China

Status. Active control on metasurfaces (MSs) is highly desired in practice, as it enables dynamical manipulations on electromagnetic (EM) waves, significantly expanding our wave-control capabilities. Tunable metasurfaces are typically realized by combining passive meta-systems with materials whose EM properties can be modulated by external knobs (e.g. temperature, voltage, electric or optical fields). Starting in 2006, many schemes were proposed to realize tunable meta-atoms at different frequency domains [129–139]. Very recently, considerable effort was devoted to making *inhomogeneous* metasurfaces with constitutional meta-atoms independently controlled by different external knobs, thereby exhibiting dynamically tuned wave-control functionalities [140–144]. However, grand challenges exist along this development, which will be briefly mentioned after we introduce the current status.

Electrically tunable meta-atoms (ETMs) have been realized at frequencies ranging from microwave to optics, thanks to versatile electrically sensitive materials available at different frequency domains, such as varactor/PIN diodes, liquid crystals (LCs), doped semiconductors and two-dimensional (2D) materials. A microwave ETM can be designed by integrating a meta-atom with a varactor/PIN diode. Through varying the bias voltage applied on the dipole, one can dynamically switch the functionality of the ETM [131, 138, 139]. However, although microwave ETMs have proven to be powerful systems to actively control EM waves, the realized devices still suffer from certain issues, such as limited working bandwidths and difficulties in transmission-mode realizations. Integrating doped semiconductors with meta-atoms is another intriguing way to get ETMs with high performances (i.e. broad bandwidth and high modulation speed). In 2009, a broadband terahertz (THz) phase modulator was experimentally demonstrated based on such a scheme (see figure 15(a)) [132]. The Schottky diode formed at the metal-semiconductor interface allows the carrier density in doped GaAs efficiently controlled by external bias voltage, resulting in real-time active amplitude (60%) and phase ($\pi/6$) modulation on the transmitted THz wave with a speed up to 2 MHz. Graphene, a 2D material with Fermi level tuned by external gating, is a good candidate to help realize ETMs. In 2012, combining gate-controlled graphene with a transmissive metasurface, Lee *et al* experimentally demonstrated active modulations on both the amplitude (47%) and phase (32.2°) of the transmitted THz wave (figure 15(b)) [133]. Very recently, an adaptive meta-lens with focal length controlled electrically, was experimentally demonstrated in optical regime based on dielectric elastomer actuators [140].

Thermal stimuli can drastically modify the EM properties of many materials. A promising approach to achieve active MSs is to hybridize MSs with thermally responsive materials, such as phase change materials (PSMs), LCs and superconductors. For instance, vanadium dioxide, a typical PSM sensitive to temperature changes, has been combined with passive MSs to achieve the 'on' and 'off' states in controlling the transmitted light. LCs with both voltage and temperature-tuned refractive index can help realize tunable MSs at different frequencies, such as tunable absorbers and spatial light modulators (see figure 15(c)) [134].

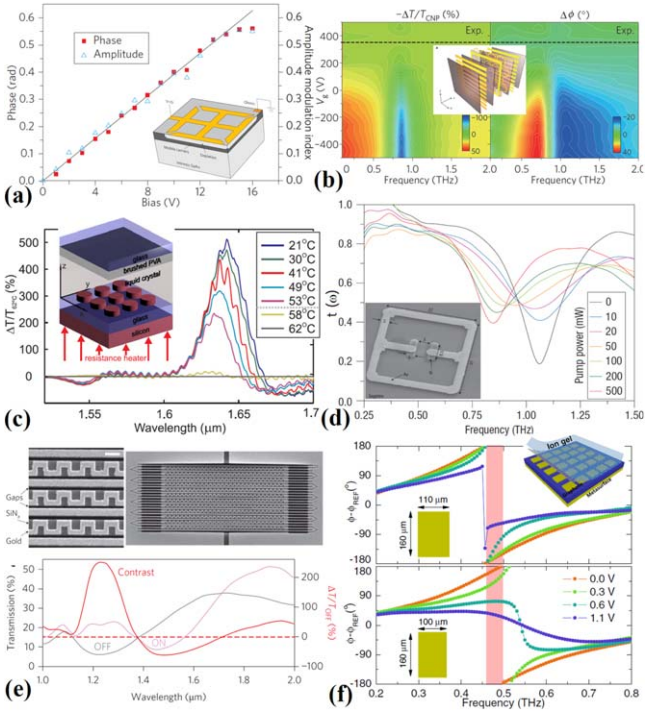

Figure 15. (a) THz phase and amplitude modulations achieved by semiconductor-hybridized ETM [132]. (b) Measured relative transmission-amplitude variation and phase change versus voltage in a gate-controlled graphene MS [133]. (c) Thermally tunable dielectric MS hybridized with LCs [134]. (d) Optically tunable MS for active amplitude control on THz wave [135]. (e) Transmission spectra of a reconfigurable MS in ON and OFF states controlled by MEMS [136]. (f) Wide-range phase tuning achieved with a gated-controlled graphene MS [137]. (a) Reprinted by permission from Macmillan Publishers Ltd: Nature Photonics [132], Copyright (2009). (b) Reprinted by permission from Macmillan Publishers Ltd: Nature Materials [133], Copyright (2012). (c) Reprinted with permission from [134]. Copyright (2015) American Chemical Society. (d) Reprinted by permission from Macmillan Publishers Ltd: Nature Photonics [135], Copyright (2008). (e) Reprinted by permission from Macmillan Publishers Ltd: Nature Nanotechnology [136], Copyright (2013). (f) Reprinted figure with permission from [137], Copyright (2015) by the American Physical Society. CC BY 3.0.

Optically tunable MSs are constructed through combining photoconductive semiconductors and passive MSs. By controlling the conductivity of the involved semiconductor through carrier photo-excitation, one can dynamically modulate the EM responses of the entire MS (see figure 15(d)) [135], leading to exotic effects such as tunable chirality and negative refraction index. Such meta-systems can offer ultrafast optical control on light but with relatively weak tunability.

Micro-electro-mechanical-system (**MEMS**) technologies have been adopted to realize reconfigurable MSs (see figure 15(e) for an example) [136], which can dynamically modulate EM waves ranging from microwave to infrared, with deformable cantilevers or thermal bimorphs frequently used to control the device configurations.

There are other materials/technologies to realize tunable MSs, such as incorporating stretchable dielectric substrate or ferrite into the MS designs, or using microfluidic technology to dynamically control the device configurations. Overall, considerable progress has been made in achieving tunable MSs based on different mechanisms, indicating the promising future of active meta-devices for diversified applications.

Current and future challenges. Achieving fully free manipulations on EM wave calls for *independent* and *full-range* control on the amplitudes and phases of local EM fields. However, most tuning mechanisms simultaneously modulate the amplitudes and phases of local EM fields. In addition, the phase-tuning ranges are much less than π in most mechanisms, which restrict their applications in designing tunable *inhomogeneous* MSs for dynamical wavefront control. Recently, a loss-driven resonance-mode-transition mechanism has been proposed to achieve wide-range phase control on EM waves, based on a complete phase diagram established for meta/insulator/metal (MIM) MSs [145]. A widely tunable THz phase modulation (>240°) was experimentally demonstrated based on gate-controlled graphene MS (see figure 15(f)) [137]. However, such wide-range phase tuning is strongly coupled with the amplitude modulation. Therefore, finding new mechanisms with amplitude and phase modulations decoupled is one grand challenge in this field.

Another major challenge is how to independently control the local EM response of each meta-atom at frequencies higher than THz. In the microwave regime, local control on individual meta-atoms is enabled by varying the bias voltage across the diode incorporated by that very meta-atom, laying a basis to realize reprogrammable meta-holograms [142] and focal-length-switchable meta-lens [141]. Recently, a THz spatial light modulator was realized based on a tunable MS with 8 × 8 pixels controlled by independent voltage biases (see figure 16(c)) [143]. However, these approaches are difficult to implement at higher frequencies, where new technologies need to be developed.

The third challenge arises from material concerns. Most tunable MSs realized so far are based on plasmonic metals, incompatibility with current CMOS technology and possessing poor chemical and thermal stabilities.

Advances in science and technology to meet challenges. New tuning mechanisms can be possibly found if one can introduce more degrees of freedom into consideration. Recent advances in nanofabrication bring promising solutions to achieve local EM control on nanometer-scale meta-atoms. For example, based on a gate-tunable conducting oxide MS, a spatial-light modulator with modulation speed up to 11 GHz

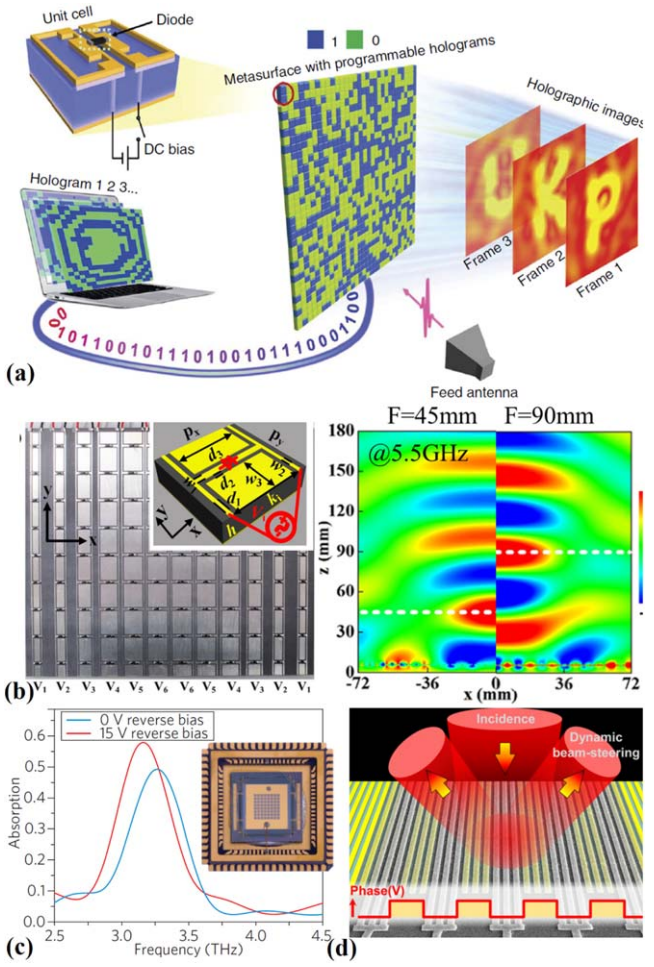

Figure 16. (a) Voltage-controlled reprogrammable meta-holograms in microwave regime [142]. (b) Tunable microwave meta-lens with switchable focal length [141]. (c) THz spatial light modulator with 8 × 8 pixels each controlled an individual bias voltage [143]. (d) Dynamical modulations on infrared-light diffractions by a gate-tunable MS with conducting oxide integrated [144]. (a) Reprinted by permission from Macmillan Publishers Ltd: Nature Photonics [142], Copyright (2017). (b) Reprinted from [141], with the permission of AIP Publishing (2016). (c) Reprinted by permission from Macmillan Publishers Ltd: Nature Photonics [143], Copyright (2014). (d) Reprinted with permission from [144]. Copyright (2016) American Chemical Society.

was recently demonstrated at telecom wavelength (see figure 16(d)) [144]. Dielectric MSs might be the solution for COMS-compatibility issue. Moreover, emerging new materials, such as transition metal nitrides (i.e. GaN, TiN) and TCOs (i.e. AZO, GZO, ITO), open up a new road to achieve COMS-compatible tunable meta-devices.

Concluding remarks. The past decade has witnessed a fast development on tunable/reconfigurable MSs. While grand challenges still exist on physics/technology/material aspects, we expect that these challenges are rather the driving forces to push the field forward, eventually making tunable/reconfigurable MSs a promising platform for realizing functional devices facing versatile application requirements.

Acknowledgments

The authors acknowledge the financial support from National Key Research and Development Program of China (Nos. 2017YFA0303504 and 2017YFA0700201), Natural Science Foundation of China (Nos. 11734007, 11474057, 11674068, 91850101), and Shanghai Science and Technology Committee (Nos. 16ZR1445200, 16JC1403100).

METASURFACES WITH HIGHER SYMMETRIES

10. Dispersive properties of periodic surfaces with higher symmetries

Guido Valerio

Laboratoire d'Electronique et Electromagnétisme, Sorbonne Université, F-75005 Paris, France

Status. The impact of specific symmetries on the dispersive properties of periodic materials is a recently emerged topic within the metamaterial research community. Symmetries of interest can be purely geometrical or involve both geometrical and temporal operators. Among the latter is the parity-time (PT) invariance: time-domain symmetries require the simultaneous presence of scatterers inducing losses and gain [146]. Despite the presence of a complex potential, PT structures support real modes [147]. Moreover, the breaking of PT symmetries can enable unidirectional propagation of states robust to small perturbations of the structure (defects, bends, etc). This can be related to the topological properties of the propagation bands of the structures [148]. Several solutions have been obtained with non-reciprocal phenomena (magnetic-field bias, gyrotropic materials). However, these structures still require a larger complexity if compared with those involving pure spatial symmetries.

Spatial symmetries in periodic electromagnetic systems were studied in the 70s in the framework of microwave waveguide [149]. Namely, *glide symmetric* waveguides were defined there as waveguides invariant under the glide operator G:

$$G: \begin{cases} x \to x + \dfrac{d}{2} \\ z \to -z \end{cases} \tag{5}$$

consisting of a translation along x and a reflection around the plane $z = 0$ (see figure 17(a)). Of course, a glide-symmetric waveguide is also d-periodic, since the translation operator T is obtained by applying twice the glide operator ($T = G^2$). The electromagnetic problem was there formulated by looking for the eigenvalues of G rather than those of T:

$$G[E_z(x, z)] = E_z\left(x + \frac{d}{2}, -z\right) = \pm e^{-jk_{x0}\frac{d}{2}} E_z(x, z) \tag{6}$$

where k_{x0} is the wavenumber of a Floquet-Bloch mode (both signs define the same mode here) [150]. The main spectral property of glide-symmetric structures discussed in [149] is the suppression of stopbands at $\beta d = \pi$, β being the modal phase constant (real part of k_{x0}) (see figure 17(b)). Another kind of spatial symmetry (*twist* or *screw symmetry*) is defined as the composition of a translation and a rotation around the periodicity axis [151], but it will not be discussed here for the sake of brevity [152].

Current and future challenges. After a few decades, the interest in glide structures has recently reawakened in connection with the development of metasurface technology. For metasurface applications, the 1D operator (5) is replaced with a 2D operator involving a translation along the directions x and y (figure 17(a)). A 2D glide symmetry is useful since it allows the synthesis of artificial media extending along two dimensions. This is particularly important for the design of graded-index planar lenses, electromagnetic band-gap materials, and 2D leaky-wave antennas [153, 154].

For a simpler presentation of the physical properties described here, we refer to the case of a 1D glide symmetry. All the results can however be simply generalized to 2D

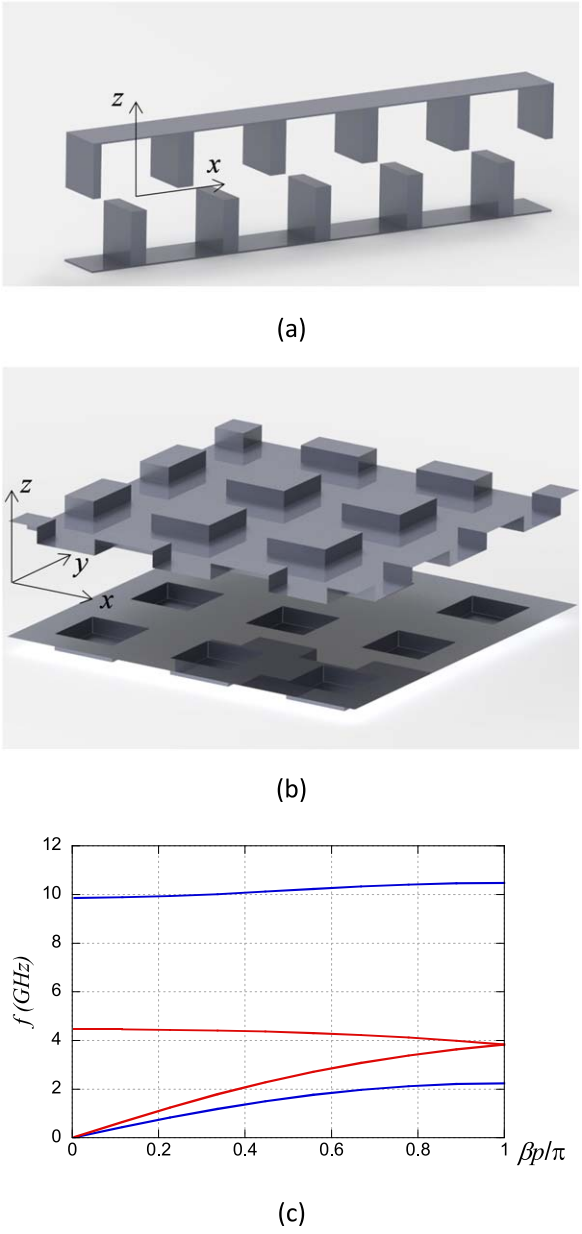

Figure 17. (a) 1D glide symmetric waveguide. (b) 2D glide symmetric structure. (c) Frequency versus phase constant of a glide (red lines) and non-glide (blue lines) structure.

configurations. A transverse-resonance approach [155] would require an equivalent homogenized model for the two surfaces. This is made difficult by the strong interaction between them, as discussed in [156]. For this reason, the standard Bloch analysis of a 1D periodic structure is formulated here as an eigenvalue problem of the transmission matrix $\underline{\mathbf{T}}$ of a single unit cell [157], if each unit cell can be described as a two-port network. Each scatterer excites a number of reactive modes, which are confined around the scatterer and do not propagate along the line. If the unit-cell boundaries are far enough from the scatterer, only the fundamental mode of the unperturbed transmission line are relevant on the ports. A 2×2 matrix is then sufficient to describe propagation along the periodic line. On each port, equivalent voltages and currents are defined (V_1, I_1 and V_2, I_2), associated with a mode of the background transmission line. A Floquet-periodicity relation at the ports of a cell is enforced:

$$\underline{\mathbf{T}} \cdot \begin{pmatrix} V_1 \\ I_1 \end{pmatrix} = \begin{pmatrix} V_2 \\ I_2 \end{pmatrix} = e^{-jk_{x0}d} \begin{pmatrix} V_1 \\ I_1 \end{pmatrix}. \tag{7}$$

This means that the unknown quantity $e^{-jk_{x0}d}$ is an eigenvalue of $\underline{\mathbf{T}}$.

If a glide-symmetry is present, the unit cell can be divided in two parts (see figure 18(b)) and we can define a $\underline{\mathbf{T}}_{1/2}$ matrix for each sub-cell. If only one mode is present at each port of the half-cell (either even or odd with respect to z), the glide operation G is equivalent to a translation apart an inessential $\pm$ sign. The eigenvalue problem (6) can be formulated as

$$\underline{\mathbf{T}}_{1/2} \cdot \begin{pmatrix} V_1 \\ I_1 \end{pmatrix} = \pm e^{-jk_{x0}\frac{d}{2}} \begin{pmatrix} V_1 \\ I_1 \end{pmatrix}. \tag{8}$$

Formulation (8) proves that, if one mode is present at the ports of a half-cell, the dispersive properties of a glide symmetric structure are the same as a structure whose period is divided by two. This clearly explains the suppression of stop-bands at $\beta d = \pi$: if the effective spatial period $d/2$ is considered, stop-bands are recovered only at $\beta d/2 = \pi$, thus at $\beta d = 2\pi$ (or, equivalently, $\beta d = 0$).

However, a more interesting case arises if a unit cell cannot be described by a 2×2 matrix, which happens if adjacent scatterers interact through higher-order modes. This is possible if they are sufficiently close and if their geometry is such that higher-order modes are effectively excited. In this case, $\underline{\mathbf{T}}^{\mathrm{d}}_{1/2}$ is a $2N \times 2N$ matrix describing one half-cell, where N modes are retained at each of its physical access ports. We can use the case $N = 2$ to highlight the effect of glide symmetry, with the two modes having different parities with respect to the glide plane $z = 0$. $V_1^{(i)}$, $I_1^{(i)}$, $V_2^{(i)}$, $I_2^{(i)}$ are the voltages and currents of the ith mode at the first and second port, respectively (see figure 18(a)).

The glide condition (6) introduces a common phasing $e^{-jk_{x0}d}$ after a translation of $d/2$, but the mirroring will also add a difference in sign for the two modes, due to their different parity in z. The eigenvalue problem in terms of the

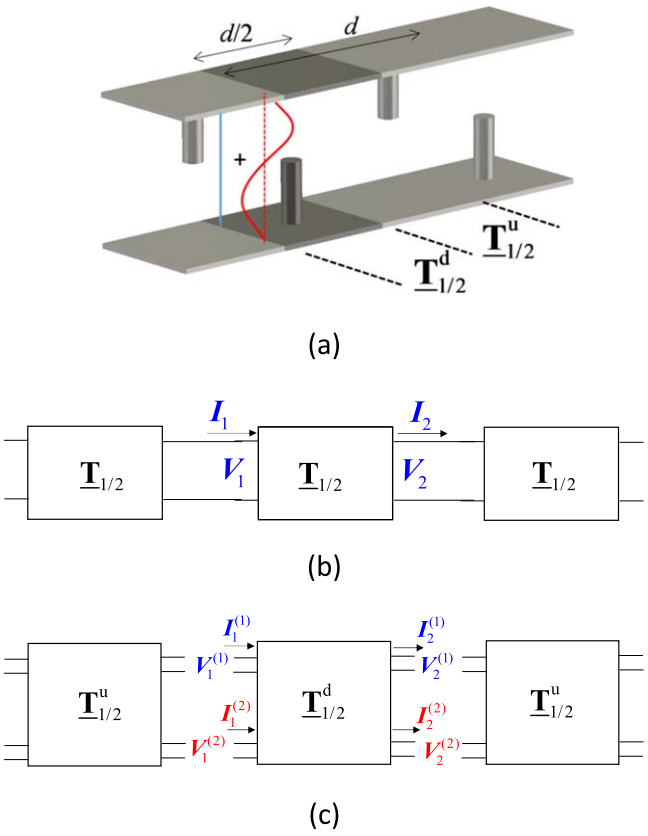

Figure 18. (a) 1D glide-symmetric pin-based metasurfaces. (b) Model retaining only one mode at each port ($\underline{\mathbf{T}}^{\mathrm{d}}_{1/2} = \underline{\mathbf{T}}^{\mathrm{u}}_{1/2} = \underline{\mathbf{T}}_{1/2}$). (c) Model retaining two modes.

$\underline{\mathbf{T}}^{\mathrm{d}}_{1/2}$ matrix becomes:

$$\underline{\mathbf{T}}^{\mathrm{d}}_{1/2} \cdot \begin{pmatrix} V_1^{(1)} \\ I_1^{(1)} \\ V_1^{(2)} \\ I_1^{(2)} \end{pmatrix} = \begin{pmatrix} e^{-jk_{x0}\frac{d}{2}} V_1^{(1)} \\ e^{-jk_{x0}\frac{d}{2}} I_1^{(1)} \\ -e^{-jk_{x0}\frac{d}{2}} V_1^{(2)} \\ -e^{-jk_{x0}\frac{d}{2}} I_1^{(2)} \end{pmatrix} \tag{9}$$

where a minus sign appears in the higher-order mode. If this higher-order mode is negligible, the glide symmetric line is equivalent to a periodic line with smaller period, as in (5). If higher-order modes are not negligible, their interactions create a fundamental difference between the glide-symmetric line and a purely periodic line with smaller period [158].

These two different cases (through the fundamental mode or through higher-order modes) are defined based on the accuracy required when solving (6). As the periodic scatterers come closer, higher-order modes become more important [159]: the definition of a threshold in the scattering parameters of the different modes can help to define which modes are relevant according to the requested accuracy.

Advances in science and technology to meet challenges. The approach discussed in the previous section has the merit of highlighting the importance of mode coupling at the unit-cell level in higher symmetric periodic structures. The suppression of the stopband at $\beta d = \pi$ also leads to the suppression of the horizontal-slope behavior typical of a band edge resonance.

This condition, together with the choice of extreme axial ratios in the unit-cell geometry, enables the propagation of waves with constant phase velocity over a ultra-wide band. The same geometries can also realize electromagnetic band-gap materials. In fact, a remarkable enhancement of the attenuation level and bandwidth in the $\beta d = 0$ stopband is obtained with respect to non-glide surfaces. Finally, glide-symmetry can increase the density of the equivalent artificial medium by reducing the fabrication precision.

It is interesting to remark that other kinds of dispersive behaviors can be obtained by introducing mode coupling in periodic lines. Namely, the coupling of two propagating and two attenuated modes defines a fourth-order degeneracy (degenerate band edge) [160]. This can be used to excite very narrowband resonances (the so-called 'giant' resonance) useful for the design of high-Q resonators [161].

These phenomena prove the interest of the study of the best topologies capable to enhance certain mode couplings, by acting both on the shape of the scatterers and on their mutual symmetries or asymmetries. New methods for homogenization and new equivalent circuit models are also required to characterize glide-symmetric structures. They are expected to take into account higher-order mode interactions, which are usually neglected in standard approaches.

Concluding remarks. We have discussed dispersion properties of higher-symmetric surfaces in terms of multiple modal couplings. Future research on this kind of phenomena can pave the way to the design of exotic dispersion behaviors.

Acknowledgments

The author wants to thank Oscar Quevedo-Teruel for important discussions on the topic. This work has been partly funded by the French Government under the ANR grant HOLeYMETA ANR JCJC 2016 ANR-16-CE24-0030.

11. Application of glide-symmetric periodic holey structures to gap waveguide technology

Eva Rajo-Iglesias

University Carlos III of Madrid, Madrid, Spain

Status. Gap waveguide technology was proposed for the first time in 2009 [162], although it was not experimentally verified until 2011 [163], but it is only now, in recent years, when the technology has finally exploded. The technology is based on the use of a periodic structure providing the boundary conditions of an artificial magnetic conductor (AMC) and its combination with a smooth metal lid to control the propagation of waves. The fundamentals of the technology are shown in figure 19(a) where the red crosses mean no propagation is allowed and the green wave represents wave propagation.

The two parts of these waveguides do not require electrical contact when assembled together, with this bringing one of its main advantages. Several realizations of this idea have been proposed and explored, the most relevant are shown in figure 19(b), namely, ridge, groove, inverted microstrip and microstrip ridge. Somehow they are equivalent respectively to conventional rectangular waveguide technology (groove) or to transmission lines (all the rest) with propagating quasi-TEM mode. Figure 19(d) shows the electric field in a cross-section of the gap waveguide versions of figure 19(c).

The main purpose of the development of this technology was to replace classical waveguide technology and printed technology when working in the millimeter frequency range. In that frequency band, the high losses of printed technology are not acceptable whilst classical waveguide technology is expensive, bulky and not flexible.

In most of the realizations presented so far in the literature, the technology uses a periodic structure to provide the AMC boundary conditions, known as a *bed of nails* surface (periodic pins shown in figure 19(c)), because it is a fully metallic periodic structure with a small periodicity and almost isotropic behavior. Its practical implementation when moving up in frequency may introduce complications due to the small dimensions of the pins (long and narrow), which can result in expensive and fragile prototypes.

Some alternatives to this implementation of gap waveguide have been proposed over the years. On one hand, the use of pins with half height has been presented in [164] (shown in figure 19(c)). The advantage of this structure is that it is able to create the same bandgap as the regular pins but with one half of its height resulting in the desired simplified manufacturing. The price to pay is the need of having two textured surfaces (top and bottom) instead of just one of them. Another option is the use of mushroom-type EBG structures as proposed in [165]. Excellent examples of the use of this version can be found in recently published works of Kishk and his group from Concordia University [166]. However, the use of this periodic structure is limited mainly to microstrip ridge version, and the presence of the dielectric definitely

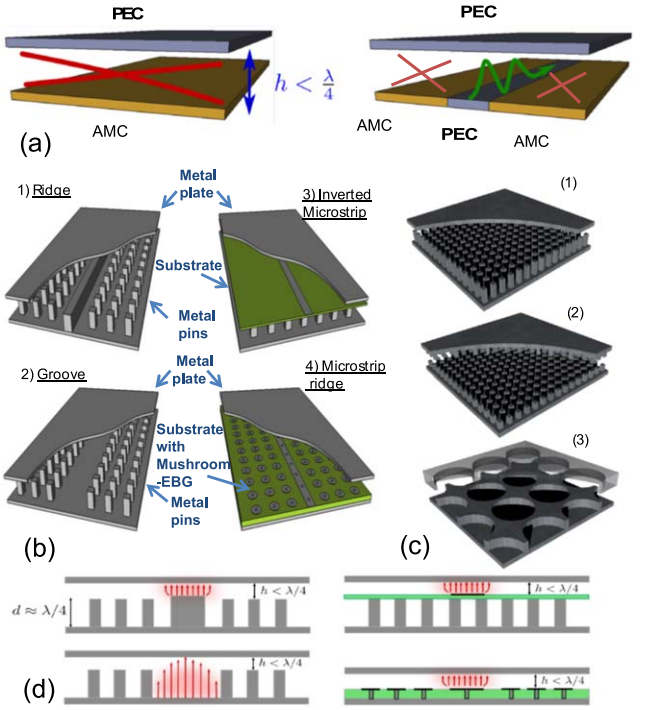

Figure 19. (a) Fundamentals of gap waveguide technology. (b) Typical realizations of gap waveguide technology using pins or mushrooms. (c) Manufacturing simplification from pins to half-pins and holes. (d) Field distribution (red arrows) in the four realizations of gap waveguide described in (b).

increases the losses. Consequently, this version is not suitable for very high frequencies.

Alternative metallic structures have been explored based on the use of holes instead of pins, whose manufacturing is much easier in nature but also its dimensions are comparatively much bigger. However, structures made of periodic holes with a smooth metal lid on top have either a very narrow stop band or directly no bandgap depending on its dimensions.

Recently, the use of higher symmetries for periodic structures applications in electromagnetism has been revisited. It was shown that by using periodic holes in a glide symmetric configuration (i.e. shifting half period and mirroring) as shown in figure 19(c), a complete stop band, i.e. an electromagnetic band gap (EBG) performance can be easily obtained in a wide frequency range. The proportional holes size with respect to equivalent pins is as shown in figure 19(c).

A complete parametric analysis of this geometry in terms of stopband was carried out in [167] with relevant conclusions to guarantee a successful use of this structure as an alternative to pins in the design of gap waveguide components. In that work, it was shown that the obtained stopbands have similar sizes as the ones with structures made with pins.

The main parameters of the structure determining its stop-band are the periodicity of the holes and their radius, in this aspect having similitudes with photonic crystals. Concerning the depth of the holes, it was demonstrated that there is a minimum required value but once that value is attained,

the structure is not sensitive to a change in this parameter. This is a relevant advantage in terms of manufacturing as when drilling holes, not accuracy or special ending is required. With this comment, we are assuming that CNC milling will be used for manufacturing as a preferred option due to its robustness, although other alternatives, such as 3D printing or stereolithography, can be also used.

Current and future challenges. The first demonstration of how this new structure can be used for designing prototypes in gap waveguide technology was presented in [154]. Its use in the groove version of the technology is quite straightforward. The designed and manufactured prototypes in U-band (shown in figure 20) have exhibited an excellent performance when verified experimentally. The gap parameter in this case can be brought to its lower limit as the decrease on that dimension makes the stopband of the structure grow. In other words, one can directly screw the two parts of the waveguide assuming no gap, but in practice small gaps will always exist and the holes will prevent any kind of leakage.

The demonstration of how to apply these glide symmetric holes as EBG still presents challenges when it is used for the design of specific waveguide components. In this sense, so far, a wideband phase shifter with potential to be reconfigurable was designed in [168] and it is also shown in figure 20. A relevant consideration is the number of required rows of holes to stop the leakage. With our experience, we have concluded that one row is sufficient for straight waveguide sections, whilst for bends or discontinuities, it is convenient to use two rows.

Another example of use of this technology is in waveguide flanges (shown in figure 20) with the purpose of avoiding any kind of losses [169] in interconnections.

The advantages of using bigger holes when compared to pins present limitations as well if we are aiming at an application where compact devices are required. For instance, in the design of array feed networks the size of the holes represents a challenge to preserve short inter-element electrical distances.

Another identified challenge is the use of glide symmetrical holes not only for the groove version of the technology [170] but also for the ridge one. Furthermore, more possibilities using other types of higher symmetries or combining several different periodic structures also have to be explored. We expect that new features apart from easy manufacturing will show up.

Advances in science and technology to meet challenges. To explode the potential of this EBG structure, bearing in mind the limitations in size, one natural step is to make antennas with this technology. Other higher symmetry periodic structures are being currently studied and it is expected that the results obtained from those investigations can be usable in some of the versions of gap waveguide technology.

Figure 20. Manufactured prototypes using glide-symmetrical holey structures. Further details can be found in [154, 167–169].

Naturally, the advances in additive manufacturing that we are experiencing day after day will be translated in a benefit for gap waveguide technology, at least at the prototyping level. Still, mass production demands simplifications in the structures without affecting the performance. In this sense, the holey structure used in combination with groove gap waveguide version has a clear future in the millimeter frequency range.

Finally, the possibility of exploring other higher symmetries and combination of different periodic structures (pins and holes, or holes/pins with different parameters) is another open research field.

Concluding remarks. Holey glide symmetrical structures have been proposed for use in gap waveguide technology with the purpose of simplifying the manufacturing at very high frequencies. Examples of the first waveguide components designed using these innovative structures have been presented. The performance in terms of stopband sizes and ability to prevent leakage are identical to the ones of periodic pins. Simplification in the manufacturing comes from the bigger dimensions of holes when compared to equivalent pins and from the simplicity of drilling holes. Nevertheless, these bigger dimensions can also be a challenge for designing some waveguide components.

Acknowledgments

This work has been partially funded by Spanish Government under project TEC2016-79700-C2-2-R and by Madrid Regional Government under project S2013/ICE-3000.

12. Quasi-analytical methods for periodic structures with higher symmetry

Zvonimir Sipus[1] *and Oscar Quevedo-Teruel*[2]

[1]University of Zagreb, Zagreb, Croatia
[2]KTH Royal Institute of Technology, Stockholm, Sweden

Status. A periodic structure possesses a higher symmetry when the unit cell coincides with itself after more than one geometrical operation of a different kind, such as translation, rotation and mirroring [171]. The combination of different types of symmetries greatly influences the propagation properties of periodic structures. For example, the dispersion of the lowest propagating mode can be significantly reduced and the band gaps can be extended or completely removed. The possibility of tailoring the dispersion diagram has enabled the design of new electromagnetic components with properties beyond the ones offered by ordinary periodic structures. Recently, it has been demonstrated that higher symmetries can be used to produce wide band Luneburg lenses [153, 172], leaky-wave antennas with low frequency dependency, cost-efficient gap-waveguide technology [154], contactless flanges with low leakage [169], low dispersive propagation in loaded co-planar waveguides, and fully-metallic reconfigurable filters and phase shifters [168]. Some of these examples are illustrated in figure 21.

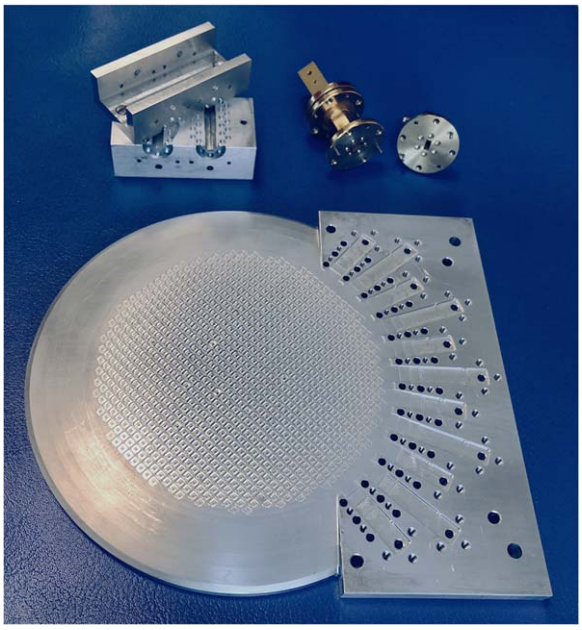

Figure 21. Realizations of glide-symmetric structures. (Bottom) Luneburg lens [172]. (Top right) Contactless flanges [169]. (Top left) Phase shifter [168].

Higher symmetries in spatial periodic structures can be of different kinds; the two most commonly used in electromagnetics are the twist and the glide types [149, 171]. A periodic unit cell possesses twist symmetry if it is repeated after a translation and a rotation, while it contains glide symmetry if the unit cell is repeated after translation and mirroring. Mathematically, we can describe such periodic structures using a combination of translation and rotation/mirroring operators [156]. Since the structure is periodic, i.e. since the field is periodic across one unit cell apart from an exponential factor describing propagation, the eigenvalue of the higher symmetry operator is the product of the eigenvalue of the translation operator (representing the phase shift through the unit cell) and the complex kth root of 1 (representing the k-fold twist symmetry; in the case of glide symmetry k is equal to 2). The corresponding eigenmode is the Bloch mode of the periodic structure, thus, the described property of structures with higher symmetry is called the generalized Floquet theorem.

The glide-symmetric structure itself, due to the mirroring operation, is compatible with fully planar geometries used in mm-wave components and integrated-circuit technology. On the other hand, twist-symmetric structures are compatible with cylindrical geometries, such as structures based on coaxial transmission lines or circular waveguides.

In order to produce a distinctive behavior in the propagating properties of higher-symmetric structures (when compared to conventional technology), a significant coupling between sub-elements is needed. This coupling is commonly achieved if the two surfaces that compose the unit cell are electrically near each other. Therefore, these unit cells will have a combination of small and large distances that typically increase the computational requirements for general tools for electromagnetic simulation. This has motivated the recent development of quasi-analytical methods to characterize these structures [150, 156, 173, 174, 175].

Current and future challenges. The first step in the design of devices containing periodic structures is the dispersive analysis of the structure, i.e. computing the wavenumber of the propagating modes. That can be done using the eigenmode analysis tool of general electromagnetic solvers. However, higher precision and reduced computational time can be obtained with specialized programs for a narrower class of electromagnetic structures which are of special relevance for practical applications. Two of the commonly used techniques for these specialized programs are circuit models and the mode-matching method.

Circuit models. The equivalent-circuit approach implements the circuit description of the unit cell geometry to establish a transmission line along the periodicity. This method was proposed in [156] to calculate the propagation constant of glide-symmetric corrugated structures. It has also been applied in [174] for a coaxial cable loaded with circular metallic inclusions, named polar-glide symmetry (figure 22(a)). The equivalent circuit provides an analytical closed-form solution, being the fastest possible method. However, it has a few disadvantages. Primarily, it is difficult to calculate the closed-form for non-canonical shapes. Furthermore, the circuits become complicated for two-dimensional periodic structures. Additionally, for complicated circuits, it is difficult to link the physical

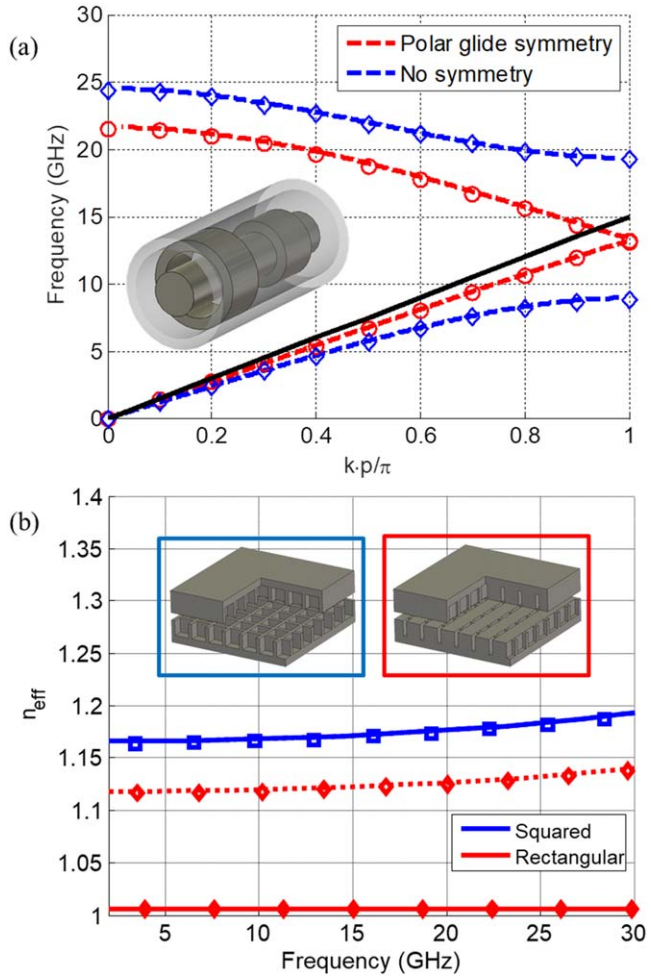

Figure 22. (a) Calculated dispersion diagram of a coaxial cable loaded with circular metallic inclusions [174]; (b) calculated effective index of refraction of a parallel-plate glide-symmetric structures [150].

properties to the circuit values. Finally, it is rather complicated to model the coupling between elements due to symmetries, and it is specifically this coupling that makes the higher-symmetric structures behave differently from common periodic structures [151].

Mode-matching. An algorithm based on the mode-matching method uses the pre-knowledge about the electromagnetic (EM) field configuration and symmetry properties to reduce the number of unknowns and to describe precisely the EM field present in the structure. This method has been employed to calculate the propagation constant in corrugated glide-symmetric structures [175], and two dimensional holey glide-symmetric structures [150, 176] (figure 22(b)). In both cases, the model resulted faster than commercial software, although slower than the aforementioned circuit models. However, the quasi-analytical solutions are easier to extrapolate to other geometries, and it is easier to identify the coupling between glide-symmetric layers. Therefore, it is easier to identify the causes of the extraordinary properties of these structures, such as low dispersion of the first mode, and the increment of the bandgap between second and third modes.

These two analysis methods (circuit models and mode-matching) require a small number of degrees of freedom to describe the EM field distribution inside the cell. Therefore, these specialized analysis approaches are faster than meshing the whole periodic unit cell with high-precision, as is done in general commercial software.

So far, the structurally-complex devices have been designed by first calculating the needed effective parameters of the considered cells and then by designing each cell separately. For example, a flat-profiled lens realized with a glide-symmetric holey structure requires a large number of slightly different cells where the required refractive index profile can be calculated using, for example, the ray-tracing approach, and can be realized by varying the hole depth or the gap between the two metallic layers. An accurate and efficient approach to optimize the whole complex structures would require a program that efficiently combines the slightly-different EM field distribution present in each cell into a global EM field distribution. The mode-matching technique can provide the amplitudes of EM field modes present in each unit cell that can be matched at the cell boundaries and, by this, a global problem has a rather small number of unknowns. In the equivalent circuit approach, knowledge of the circuit parameters of a unit cell leads to a straightforward evaluation of the whole structure by considering a cascade of unit cells; such an approach can be generalized to a two-dimensional lattice [177].

Concluding remarks. Topics that need to be addressed related to the development of analysis methods for higher-symmetric structures include:

1. Analysis and design of dielectric structures with higher-order symmetry.
2. Developing circuit-models and mode matching models for different realizations of structures with higher symmetry.
3. Developing circuit models that accurately include the mutual coupling between the cells. The existing circuit models were developed for weakly coupled waveguide structures.
4. Developing an efficient way of combining a large number of mode-matching sub-problems into a global electromagnetic problem; investigating different iterative methods suitable for the mode matching procedure.

Acknowledgments

The authors would like to thank Professor Guido Valerio for his inspiring and helpful discussions, as well as Qiao Chen for supporting with part of the simulations represented in figure 22.

NUMERICAL AND ANALYTICAL MODELLING OF METASURFACES

13. Analysis of metasurfaces via an equivalent circuit approach

Francisco Mesa, Raúl Rodríguez-Berral and Francisco Medina

University of Sevilla, Spain

Status. The current theory and practice of metasurfaces have an important precedent in the planar periodic or quasi-periodic arrays of printed patches (or the complementary structure of apertures in a metallic screen) commonly used in microwaves and antenna engineering; for instance, frequency selective surfaces (FSSs) [178] and reflectarrays/transmitarrays [179]. A common characteristic of the scatterers of these periodic structures is that their size is of the order of the wavelength at the operation frequencies (namely, the frequency operation band usually involves, at least, the fundamental resonance of the isolated scatterers). This feature makes it that the rigorous electromagnetic analysis of the structures has to resort to full-wave computational methods demanding high computational resources. However, an alternative approach that requires much lower computational resources but still provides sufficiently accurate results, along with a good qualitative physical insight of the electromagnetic scattering phenomena, is the equivalent circuit approach (ECA) [180–183]. This approach was firstly applied to deal with planar discontinuities inside hollow metallic waveguides [180], and it was soon recognized to be extendable to discontinuities inside a generalized waveguide [184]. Here, it should be reminded that the scattering of an incident plane wave on an FSS can alternatively be considered as the problem of a patch (aperture) discontinuity inside a virtual waveguide formed by the boundaries of the unit cell (under normal incidence, the walls of a symmetric unit cell are perfect electric and/or magnetic walls, which turn into periodic boundary walls for oblique incidence [184]). The application of the ECA to the study of FSSs has shown that a few reactive elements are often capable of appropriately accounting for the complex electromagnetic behavior of these structures.

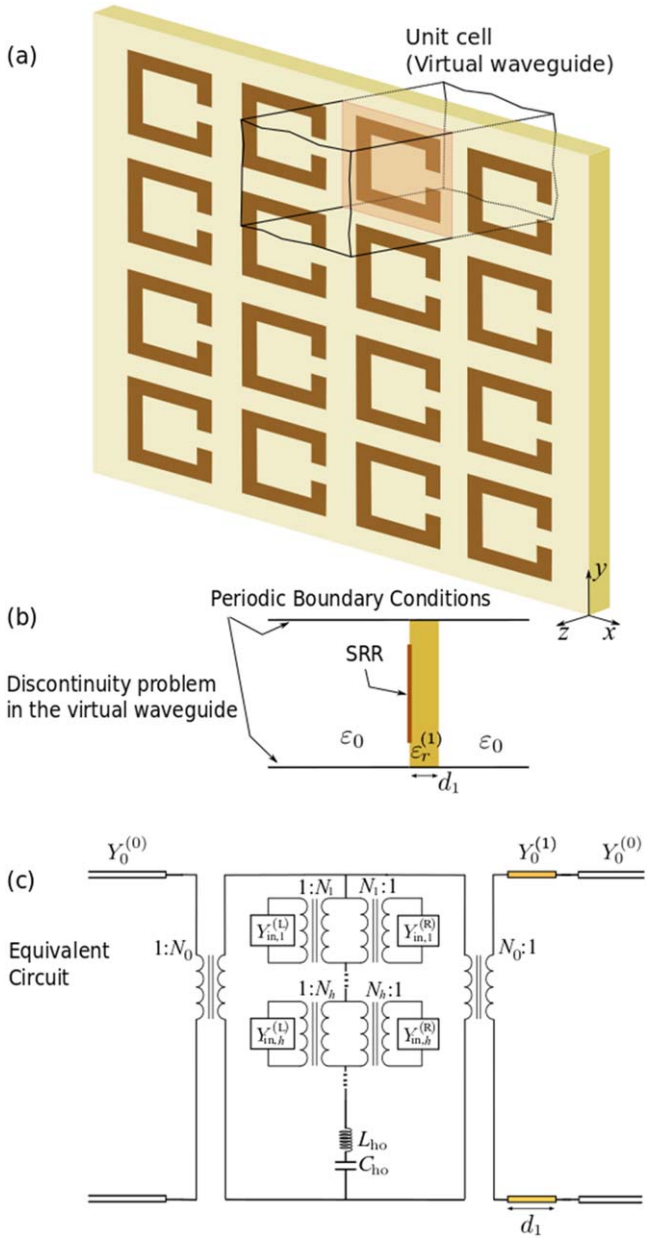

Figure 23. (a) Metasurface under study. (b) Transverse view of the equivalent electromagnetic problem. (c) Equivalent circuit.

Current and future challenges. The authors of the present work in collaboration with other researchers have been contributing to the development and application of the ECA in the last decade. Some of these contributions are, for instance, the explanation of the so-called extraordinary optical transmission in terms of a very simple equivalent circuit (actually a simple LC tank with an explicit frequency dependency included in the capacitance), the derivation of phase resonances in compound gratings by means of a simplified network of static capacitances, a systematic multimodal network to deal with 1D and 2D arrays of patches/apertures embedded in a layered environment with closed-form expression for all of the elements involved in the circuit, explanation of induced transparency through metallic screens, appearance of backward-wave bands in negative-index fishnet structures and so on (see [183] and references therein). In the application of the ECA to the structures under study, it is crucial to pay attention to the limits of validity of the ECA. In our experience, this validity range extends up to frequencies below the second excitable resonance of the isolated scatterers [185]. Also, non-negligible thicknesses of the patches/apertures of the order of (or greater than) a tenth of the operation wavelength are not easily accounted for by the ECA. It means that those periodic or quasi-periodic planar arrays reported in the literature with large electrical size of the scatterers and/or non-negligible thickness are not readily

amenable to be dealt with the ECA [183]. Fortunately, metasurfaces are usually made up of scatterers with not such a large electrical size and/or thickness and thus they are good candidates to be studied with the ECA. Up to now, not many researchers have exploited this potentiality of the ECA [186] and the present work will try to briefly illustrate the benefits of this approach for the design/analysis/synthesis of metasurfaces.

Advances in science and technology to meet challenges. As already stated, the scattering problem under consideration (see figure 23(a)) reduces the analysis of the scattering of a planar metallic discontinuity inside a virtual waveguide with periodic-boundary walls (figure 23(b)). Clearly, this problem can be solved using Bloch analysis; namely, the modes of the virtual waveguide are the Bloch harmonics. Starting from this modal analysis, an integral equation can be posed for the tangential electrical field in the metallic discontinuity. Assuming that the current density in the metallic scatterer can be factorized in the following way [185],

$$\mathbf{J}(x, y; \omega) = F(\omega)\mathbf{j}(x, y) \tag{10}$$

and imposing power conservation through the discontinuity, it is possible to write the reflection coefficient associated with the incident plane wave as

$$R = \frac{Y_0^{(0)} + Y_{\text{in},0}^{(R)} - |N_0|^2 Z_{\text{eq}}^{-1}}{Y_0^{(0)} + Y_{\text{in},0}^{(R)} + |N_0|^2 Z_{\text{eq}}^{-1}} \tag{11}$$

where

$$Z_{\text{eq}} = \frac{1}{j\omega C_{\text{ho}}} + j\omega L_{\text{ho}} + \sum_{h=-M}^{M} \frac{|N_h|^2}{Y_h^{(0)} + Y_{\text{in},h}^{(R)}} \tag{12}$$

with the different quantities above being defined in [185] and corresponding to the topology shown in figure 23(c). The transmission coefficient can then be computed following the standard line-transmission theory. A relevant point here is that the transformer ratios N_h employed above are found to be given in terms of the Fourier transform (FT) of the assumed spatial profile in the scatterers, $\mathbf{j}(x, y)$, so that

$$N_h = \tilde{\boldsymbol{j}}^{*}(\mathbf{k}_{\text{t},h}) \cdot \hat{\mathbf{v}}_h \tag{13}$$

where the symbol $\tilde{}$ stands for FT with respect to x, y and $\hat{\mathbf{v}}_h$ is defined in [185]. Since the spatial profile $\mathbf{j}(x, y)$ has been assumed to be frequency independent, it means that the FT operation only has to be done once. For canonical geometries (such as rectangular and circular ones), one can take a good closed-form mathematical guess for this profile [183] and thus its corresponding FT can also be obtained in closed form. However, for scatterers of arbitrary geometry, it is possible to obtain this spatial profile from one single computation of the full-wave simulator or even as the lowest-order eigenmode of the hollow-pipe waveguide formed by the boundaries of the scatterer [185] (this last procedure involves the solution of a 2D eigenproblem for which many efficient procedures have been reported in the literature). Once the spatial profile is computed, the transformer ratio can be numerically obtained by applying fast-Fourier-transform techniques. The results of applying this method to the structure shown in figure 23(a) and already treated in [187] are shown in figure 24. This figure shows a good agreement between our results and those reported in [187] at the resonance region. This agreement deteriorates for higher frequencies close to the second resonance of the SRR where our simplified assumption of the factorization carried out in equation (10) is no longer valid. However, it should be pointed out that within the large range of applicability of the ECA, this procedure provides accurate results with a very reduced CPU effort.

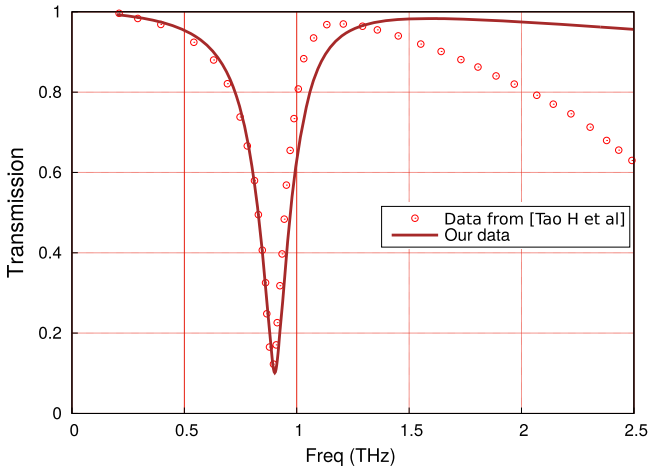

Figure 24. Transmission for the metasurface made up of split ring resonators already studied in [187].

Concluding remarks. The bottom line of this work is that the quasi closed-form ECA is a very efficient tool to study metasurfaces providing that the frequency band of interest lies inside the limit of validity of the approach. This validity frequency range extends up to close the second resonance of the individual scatterer of the periodic metasurface, which covers many practical situations of interest.

Acknowledgments

This work has been supported by the Spanish Ministerio de Economía y Competitividad with European Union FEDER funds (project TEC2017-84724-P).

14. New perspectives on the modeling of metasurfaces

Ana Díaz-Rubio, Victor Asadchy and Sergei Tretyakov

Department of Electronics and Nanoengineering, Aalto University, Aalto, Finland

Status. In the last decade, research on metasurfaces has revealed their unique properties, promising numerous applications in optics and microwave engineering. Metasurfaces are thin layers composed of polarizable inclusions with electric, magnetic or, in a more general case, bianisotropic responses. These inclusions are usually small in comparison with the wavelength in the surrounding medium, opening up the possibility to use homogenization theories for their analytical modeling and design. Through averaging the tangential fields and induced polarizations, homogenization theories allow description of the electromagnetic properties of metasurfaces by effective parameters, like sheet impedances, susceptibilities, or collective polarizabilities. Homogenization models are powerful tools for the design of functional metasurfaces, allowing us to predict and optimize their electromagnetic response or, using an inverse approach, design the structures that provide the desired response for specific excitations.

As compared with thin layers of conventional materials, the main difference (which in fact enables new and interesting effects) is that the sizes of unit cells, a, are not negligibly small with respect to the wavelength, λ. This allows effects of weak spatial dispersion, such as artificial magnetism (second-order spatial dispersion, $(a/\lambda)^2$) and magnetoelectric coupling (reciprocal bianisotropy effects produced by first-order spatial dispersion, (a/λ)). Analytical models of artificial magnetism are simple, as the corresponding effects are similar to those in layers of conventional magnetic materials (although we should remember that spatial dispersion effects are reciprocal). Other weak spatial dispersion effects which can be modeled using effectively local sheet parameters (not invoking spatial derivatives of the fields) are the bianisotropy effects of chirality and omega coupling [188]. Also, nonreciprocal magnetoelectric effects of artificial velocity and the Tellegen effect can be modeled by effectively local relations, properly linking the tangential field components on the two sides of the metasurface.

The use of bianisotropy has opened possibilities for asymmetric control of the reflection phase with omega-coupling (reciprocal) or transmission phase with the Tellegen effect (non-reciprocal). In order to design bianisotropic metasurfaces, analytical models based on polarizabilities (relating local fields and surface polarization densities), susceptibilities (relating averaged fields and surface polarization densities) or equivalent impedance matrices are commonly used. Each homogenization model has different advantages. For example, the polarizability-based model allows calculation of the required polarizabilities of the individual particles. On the other hand, the values of susceptibilities immediately tell if the metasurface is lossy or active. Finally, the impedance matrix representation is a powerful tool for the analysis of a cascade of metasurfaces using the transmission-line approach. Detailed descriptions of these homogenization methods can be found in [189].

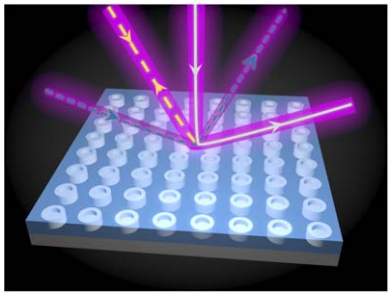

Figure 25. Schematic representation of a multichannel metasurface.

Recently, the concept of metasurfaces has been extended to non-homogenizable metasurfaces [48, 190–195]. For instance, metasurfaces where the distances between inclusions are subwavelength but the structural periodicity allows the excitation of higher-order Floquet modes required novel approaches to modeling. The evolution of gradient metasurfaces has been fast in the last few years and many studies have been focused on phase-controlling metasurfaces [48, 190–194], bianisotropic metasurfaces [188] or strongly non-local metasurfaces for wavefront manipulations [190–193]. For the analysis and practical realizations of such metasurfaces, it is important to distinguish between the macroscopic and mesoscopic responses of the metasurface. The macroscopic behavior refers to the scattering properties of the whole non-uniform structure, for example, the energy distribution between Floquet modes. The mesoscopic properties are studied considering each unit cell of a gradient metasurface in a periodical lattice of identical cells (the locally-periodic approximation).

A remarkable possibility opened up as an extension of gradient metasurfaces to multichannel metasurfaces (figure 25). In such metasurfaces, each Floquet mode is considered as a channel of an N-port device [190]. By controlling the structural periodicity, it is possible to define the number of 'channels' in the system. The electromagnetic properties of the metasurface define the scattering response for the illumination coming from different channels. A useful tool for describing multichannel metasurfaces is the scattering matrix, but estimating its components is not an easy task.

Advances in science and technology to meet challenges. With the development of metasurfaces, new challenges are emerging due to the limitations of the current modeling tools, especially in the analysis of non-uniform or gradient metasurfaces. Although the most interesting and useful effects appear due to spatial dispersion (non-local response) of the metasurface unit cells, the known modelling methods can be applied only when the spatial dispersion is weak (artificial magnetism and bianisotropy). In the other extreme, when the unit cells have the sizes of the order of the wavelength or larger, the diffraction grids theory can be used. We need to develop reasonably simple but enough accurate

models of mesoscopic metasurfaces, where the spatial dispersion effects go beyond those which can be accounted for using expansion terms of the order of (a/λ) or $(a/\lambda)^2$. Apparently, the appropriate metasurface transition conditions should explicitly involve spatial derivatives of the fields. Higher-order impedance boundary conditions are known for layers of conventional materials, but the community has not yet found an effective way to create such models for metasurfaces with complex and resonant responses.

Another challenge is that by using the available modeling tools, it is not possible to fully understand and design an *N*-channel metasurface. Currently, designs of the desired response of the metasurface under a specific illumination uniquely define the required metasurface parameters. Is it possible to find the electromagnetic properties that provide at the same time different responses for different illuminations? Although at this time there is no definite answer to this question, based on the scenarios analyzed in [190], one can deduct that the role of evanescent fields is critical in these applications.

An important limitation follows from the local-response assumption in the analysis and implementation process of gradient metasurfaces. This assumption greatly simplifies the design procedure [194, 195], but it has been demonstrated in [191] that the implementation of metasurfaces with certain macroscopic features may require strong non-local behavior, due to the necessity to guide the energy along the metasurface. The absence of modeling tools that deal with strong non-locality makes the use of numerical optimization tools necessary. For applications such as metasurface-based antennas, where complex wavefront transformations are required, the complex electromagnetic properties of the metasurface will require many deeply subwavelength elements, complicating the design and fabrication. The question that we arrive at is: is it possible to include a strong non-local response in the analytical models and control the macroscopic response by defining the electromagnetic properties of a few elements and coupling between them? Some advances have been done towards this end in [192, 193]. However, the applicability of such methods is still limited to basic scenarios for plane wave manipulation.

Another challenge is related to recently conceptualized space-time modulated metasurfaces (figure 26). Modulating inhomogeneous metasurfaces in time allows new important functionalities, especially in creating and engineering non-reciprocal response without the use of external magnetic bias. Currently, many of the studies of time-modulated metasurfaces are based on over-simplified models of time-dependent static permittivity [196–198]. This approach is not valid if the unit cells exhibit frequency dispersion and have resonances in the frequency range of interest. While conventional time-space modulated devices (like travelling-wave tubes) can be modelled with this assumption, useful functionalities of metasurfaces are enabled by the resonant behavior of unit cells. Thus, more advanced modelling methods need to be created.

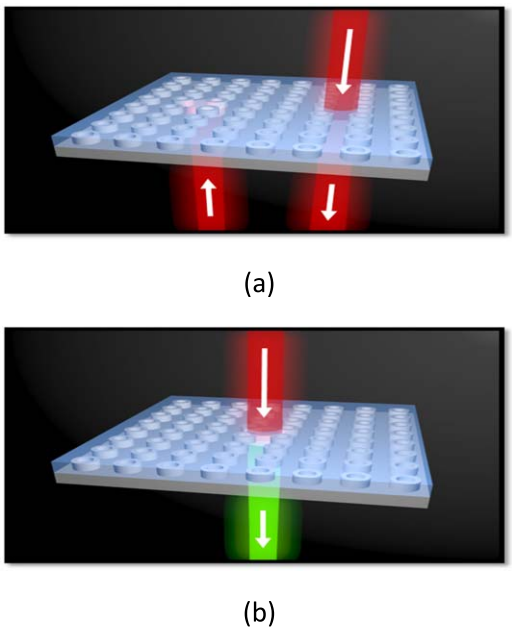

Figure 26. Possibilities for space-time modulated metasurfaces. (a) Non-reciprocal metasurfaces. (b) Frequency converters.

Concluding remarks. As we have outlined above, research and development of metasurface devices follows the line of using more and more complex structures of the unit cells, including non-reciprocal, time-dependent, and even active elements. On the other hand, researchers play with complex gradient metasurfaces which have resonant response of unit cells and at the same time space-modulation periods comparable with the wavelength. Some features of such complex metasurfaces can be revealed using numerical simulations, but it is clear that we need more advanced analytical models to interpret, design, and fully exploit the properties of emerging metasurfaces.

Acknowledgments

This work was supported by the Academy of Finland (projects 13287894 and 13309421).

15. Numerical methods for metasurfaces, with focus on method of moments

Christophe Craeye

Université Catholique de Louvain, Belgium

State of the art. As is the case in many fields of engineering, besides conceptual thinking, which will always remain essential for developing creative solutions, the role of numerical methods is increasingly important. Indeed, they are useful to rapidly validate new concepts and also to efficiently optimize initial designs. In the case of development of metasurfaces, those methods yield full-wave solvers for electromagnetic fields. In the majority of cases, the considered geometries correspond to metallizations printed on or inside layered media. Those media can be planar, but they can also cover cylinders or spheres; they may also be extended to become conformal to objects with arbitrary shapes, such as cars and aircraft.

Maxwell's equations can be solved either in the time domain or in harmonic regime. One may also try to solve them in their differential form or integral form; the latter expressing fields in a given region as a radiation integral over a given source distribution. This yields four categories of methods. Finite differences and finite elements, as well as finite integration (which presents some similarities with finite differences), are generally used for solving equations in differential form. Regarding the integral-equation formulation, the method of moments (MoM) is clearly the most popular technique. It is generally confined to fields in the harmonic regime, since time-domain solutions remain a challenge from stability and memory points of view. This section will mainly focus on integral-equations approaches—and hence on MoM—since they avoid the use of absorbing boundary conditions and, more importantly, rely on a vast heritage of analytical techniques—in particular Green's functions [199]—which makes them often more efficient and allows analytical reasoning. Specific to metasurfaces is the use of specialized boundary conditions, which go beyond what is known for interfaces between 3D homogeneous media. These are generally modelled as generalized sheet transition conditions (GSTCs) [200, 201] and relate the difference between tangential electric and magnetic fields on both sides of the metasurface to electric and magnetic surface polarization densities, themselves linearly related to the sum of fields on both sides of the metasurface. Impedance boundary conditions (IBCs) [202] may be viewed as a special case of the GSTCs (see the example in figure 27 for a metasurface antenna).

For the development of metasurfaces, numerical methods play an essential role in three areas. First, they may quantitatively guide the homogenization process, i.e. the representation of textured surfaces by (generally anisotropic) GSTCs; this is often done based on a local periodicity assumption. Second, they allow the fast solution of fields on metasurfaces represented with equivalent impedance boundary conditions (sheet impedances or GSTCs). Third, they

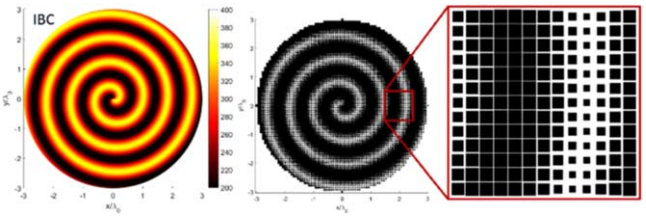

Figure 27. Impedance boundary condition for a metasurface antenna radiating a pencil beam at broadside. (Left) Homogenized representation. (Middle, right) Implementation with metallic patches printed on a grounded substrate.

enable the validation of the performance of the physical metasurface structure, while accounting for the fine details of the final geometry.

The MoM applied to surface integral equations considers piecewise homogenous media and aims at estimating equivalent electric and magnetic currents at every interface [203, 204]. Those currents are discretized into a number of basis functions, with coefficients found by imposing the boundary conditions. The latter correspond to the continuity of tangential electric and magnetic fields for standard materials or GSTCs across the metasurface sheet. A vast analytical background can be exploited to link currents with radiated fields, in the form of Green's functions associated with a given environment, such as a planarly layered medium. In particular, when a local periodicity assumption is made, fields are solved in a unit cell and the periodic Green's function accounts for the 'phase-shifted copies' of the source in all cells. Over the years, the computation of those functions has been tremendously accelerated [203], beyond the initial Floquet-wave decompositions (Fourier series accommodating linear phase shift). After inclusion of those Green's functions in the MoM, efficient methods have been developed for determining the dispersion curves of the periodic media, that is, for any frequency, the inter-cell phase shifts (or transverse Bloch wavenumbers) for which eigenmodes may occur.

Once the texture of the metasurface has been homogenized, the integral equation can be reformulated by exploiting equivalent IBCs, which are inherently spatially dispersive (dependent on transverse wavenumbers). That new equation can be solved in a traditional way, e.g. making use of local basis functions. However, since the surface impedance or sheet impedance is usually a smooth function defined on a canonical domain, e.g. a disk, one can use entire-domain basis functions to describe the unknown currents. This has been done in [205–208], with a drastic reduction of the total number of unknowns, leading to a system of equations that can be solved directly within a couple minutes on a desktop computer (see figure 28). Finally, the approximations inherent to the homogenization step may be checked by running a full-wave solution for the final metasurface, described with its detailed inclusions or printed patches. Here too, one can rely on a vast heritage of acceleration techniques developed for instance for the analysis of microwave printed-circuit boards. Two categories of accelerations are generally found. The first one concerns the reduction of the number of unknowns through the

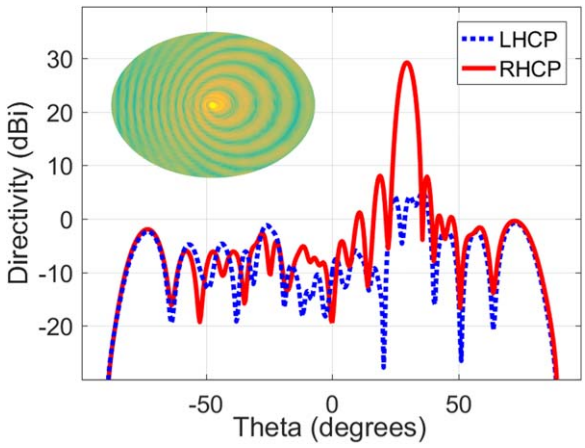

Figure 28. From [207]: current distribution and radiation patterns for an elliptical metasurface with size 7.6 × 5.4 wavelengths. Analyzed with Fourier-Bessel whole-domain basis functions.

'aggregation' of elementary basis functions. That approach relies on the fact that, even if the cells exhibit very fine details, the number of significant degrees of freedom of the induced current is limited to 2 to 4 if the cell is very small compared to the wavelength. Those 'macro basis functions' can be obtained on both numerical and analytical bases [209, 210]. The other acceleration is more numerical in nature, but it also relies on analytical techniques. It appears in the iterative solution of very large systems of equations and corresponds to the fast evaluation of fields at the interfaces for a given current distribution (or corrective term). This acceleration often makes use of the either the fast Fourier transform [211] or of the multipole decomposition of Green's function [212]. It is of course possible to combine aggregation and fast iterative techniques, leading to accelerations by two to three orders of magnitudes, as compared to the 'classical' MoM (say from the early 1990s) [202, 209].

Current and future challenges. The previous paragraph may leave the impression that metasurface researchers are 'all set' from a numerical point of view and that, from now on, one may mainly rely on Moore's law applied to computing hardware. That would be overlooking quite a few short to long-term challenges.

In the short term, it is desirable to accelerate the full-wave simulation of very large metasurfaces, with diameters larger than 20 wavelengths and to speed up the determination of eigenmodes. Regarding the latter, the search for eigenmodes generally amounts to searching for zeros of the determinant of the MoM matrix obtained for periodic structures. It is expected that, while striving towards new properties, the metasurfaces may become quite complex, with 3-dimensional inclusions and multiples layers. In this context, one should be careful about including high-order Floquet modes in the analysis: very high orders are necessary to study a given layer, while moderate orders ('accessible modes' [213]) are needed to analyze the interaction between consecutive layers.

In the medium term, improved numerical methods should be developed to support the efforts toward wideband and reconfigurable metasurfaces. Special care also needs to be given to the design of the feeding structure or 'surface-wave launcher', as well as control lines for reconfigurable metasurfaces. Indeed, those may challenge the local periodicity assumption as well as the homogenization process itself. For reasons related to space and frequency allocation, metasurfaces will almost certainly be exploited for other purposes, and can be used in extreme circumstances, e.g. in space applications. This calls for a multi-physics approach to metasurface analysis.

In the long term, some fundamental assumptions made in the MoM for metasurface analysis will certainly get challenged. Probably the most important ones come from the use of specific Green's functions, e.g. describing fields in planarly or cylindrically layered media. What if those media do not have such canonical shapes? This becomes an issue when the metasurfaces need to be made conformal. At this point, the most obvious answer consists of using methods solving Maxwell's equations in differential from, such as FEM, FDTD [204] and the finite integration technique (FIT), or a more general form of surface integral equations, where both the substrates and the metallizations need to be discretized (time-domain techniques may also prove essential for the analysis of non-linear metasurfaces). Another issue arises when a planar substrate is truncated. This problem may appear when the size of the metasurface needs to be minimized and that surface-wave phenomena are exploited, in which case scattering at the end of the substrate cannot be neglected. Although some corrections exist for scattering by the edges of a substrate, their application may become cumbersome or inaccurate when complex shapes are envisaged. At this point, it is difficult to say whether the above challenges will be solved by resorting to completely different methods, such as FDTD [204], FIT or FEM or whether accurate extensions of the MoM will be found for those new configurations. In the author's opinion, new differential-equation based techniques will certainly help, but probably the most important advances will come from extended forms of the MoM. Indeed, to understand how metasurfaces should look like in those new configurations, new analytical approaches regarding creeping waves and Green's functions for more complex bodies should be found. Then, the MoM should again be able to inherit from those new analytical tools, and in turn provide faster and more accurate solutions for fields guided or radiated by conformal metasurfaces on complex supports.

Acknowledgments

The author thanks Modeste Bodehou and Simon Hubert from UCLouvain for their inputs and comments.

ORCID iDs

Oscar Quevedo-Teruel https://orcid.org/0000-0002-4900-4788
Hongsheng Chen https://orcid.org/0000-0003-3573-3338
Ana Díaz-Rubio https://orcid.org/0000-0002-0115-1834
Nikitas Papasimakis https://orcid.org/0000-0002-6347-6466
Andrea Alù https://orcid.org/0000-0002-4297-5274
Guido Valerio https://orcid.org/0000-0003-4372-2858
Eva Rajo-Iglesias https://orcid.org/0000-0002-8012-9802

References

[1] Gok G and Grbic A 2013 Tailoring the phase and power flow of electromagnetic fields *Phys. Rev. Lett.* **111** 233904
[2] Gok G and Grbic A 2014 A printed antenna beam former implemented using tensor transmission-line metamaterials *IEEE Int. Symp. on Antennas and Propagation (Memphis, TN)*
[3] Tierney B B, Limberopoulos N I, Ewing R and Grbic A 2018 A planar, broadband, metamaterial-based, transmission-line beamformer *IEEE Trans. Antennas Propag.* **66** 4844–53
[4] Raeker B and Grbic A 2018 Paired metasurfaces for amplitude and phase control of wavefronts *IEEE Int. Symp. on Antennas and Propagation (Boston, MA)*
[5] Minatti G, Faenzi M, Martini E, Caminita F, De Vita P, González-Ovejero D and Maci S 2015 Modulated metasurface antennas for space: synthesis, analysis and realizations *IEEE Trans. Antennas Propag.* **63** 1288–300
[6] Nicholls J and Hum S V 2016 Full-space electronic beam-steering transmitarray with integrated leaky-wave feed *IEEE Trans. Antennas Propag.* **64** 3410–22
[7] Pfeiffer C and Grbic A 2015 Planar lens antennas of subwavelength thickness: collimating leaky-waves with metasurfaces *IEEE Trans. Antennas Propag.* **63** 3248–53
[8] Epstein A, Wong J P and Eleftheriades G V 2016 Cavity-excited Huygens' metasurface antennas for near-unity aperture illumination efficiency from arbitrarily large apertures *Nat. Commun.* **7** 10360
[9] Epstein A and Eleftheriades G V 2016 Arbitrary power-conserving field transformations with passive lossless omega-type bianisotropic metasurfaces *IEEE Trans. Antennas Propag.* **64** 3880–95
[10] Pereda A T, Caminita F, Martini E, Ederra I, Teniente J, Iriarte J C, Gonzalo R and Maci S 2018 Experimental validation of a Ku-band dual-circularly polarized metasurface antenna *IEEE Trans. Antennas Propag.* **66** 1153–9
[11] Ranjbar A and Grbic A 2018 Multifunctional all-dielectric metasurfaces *IEEE Int. Symp. on Antennas and Propagation (Boston, MA)*
[12] Hum S V and Perruisseau-Carrier J 2014 Reconfigurable reflectarrays and array lenses for dynamic antenna beam control: a review *IEEE Trans. Antennas Propag.* **62** 183–98
[13] Perez-Palomino G, Baine P, Dickie R, Bain M, Encinar J A, Cahill R, Barba M and Toso G 2013 Design and experimental validation of liquid crystal-based reconfigurable reflectarray elements with improved bandwidth in F-band *IEEE Trans. Antennas Propag.* **61** 1704–13
[14] Tichit P H, Burokur S N, Germain D and De Lustrac A 2011 Design and experimental demonstration of a high-directive emission with transformation optics *Phys. Rev.* B **83** 155108
[15] Mencagli M Jr, Martini E, Gonzàlez-Ovejero D and Maci S 2014 Metasurface transformation optics *J. Opt.* **16** 125106
[16] Li M and Behdad N 2013 Wideband true-time-delay microwave lenses based on metallo-dielectric and all-dielectric lowpass frequency selective surfaces *IEEE Trans. Antennas Propag.* **61** 4109–19
[17] Liang L and Hum S V 2016 Design of a UWB reflectarray as an impedance surface using Bessel filters *IEEE Trans. Antennas Propag.* **64** 4242–55
[18] Wu Z, Ra'di Y and Grbic A 2017 A tunable polarization rotator based on metasurfaces *11th European Conf. on Antennas and Propagation (EUCAP) (Paris)* pp 728–30
[19] Fong B H, Colburn J S, Ottusch J J, Visher J L and Sievenpiper D F 2010 Scalar and tensor holographic artificial impedance surfaces in *IEEE Trans. Antennas Propag.* **58** 3212–21
[20] Minatti G, Maci S, De Vita P, Freni A and Sabbadini M 2012 A circularly-polarized isoflux antenna based on anisotropic metasurface in *IEEE Trans. Antennas Propag.* **60** 4998–5009
[21] Pereda A T *et al* 2018 Experimental validation of a Ku-band dual-circularly polarized metasurface antenna in *IEEE Trans. Antennas Propag.* **66** 1153–9
[22] Li M, Xiao S, Long J and Sievenpiper D F 2016 Surface waveguides supporting both TM mode and TE mode with the same phase velocity in *IEEE Trans. Antennas Propag.* **64** 3811–9
[23] Minatti G, Caminita F, Martini E, Sabbadini M and Maci S 2016 Synthesis of modulated-metasurface antennas with amplitude, phase, and polarization control in *IEEE Trans. Antennas Propag.* **64** 3907–19
[24] Minatti G *et al* 2015 Modulated metasurface antennas for space: synthesis, analysis and realizations in *IEEE Trans. Antennas Propag.* **63** 1288–300
[25] Minatti G, Faenzi M, Sabbadini M and Maci S 2017 Bandwidth of gain in metasurface antennas in *IEEE Trans. Antennas Propag.* **65** 2836–42
[26] Smith D R, Yurduseven O, Mancera L P, Bowen P and Kundtz N B 2017 Analysis of a waveguide-fed metasurface antenna *Phys. Rev. Appl.* **8** 054048
[27] Sievenpiper D F 2005 Forward and backward leaky wave radiation with large effective aperture from an electronically tunable textured surface in *IEEE Trans. Antennas Propag.* **53** 236–47
[28] Yurduseven O, Marks D, Fromenteze T and Smith D 2018 Dynamically reconfigurable holographic metasurface aperture for a Mills-Cross monochromatic microwave camera *Opt. Express* **26** 5281–91
[29] Ahmed A, Goldthorpe I A and Khandani A K 2015 Electrically tunable materials for microwave applications *Appl. Phys. Rev.* **2** 011302
[30] Debogović T, Bartolić J and Perruisseau-Carrier J 2014 Dual-polarized partially reflective surface antenna with MEMS-based beamwidth reconfiguration in *IEEE Trans. Antennas Propag.* **62** 228–36
[31] Fong B H, Colburn J S, Ottusch J J, Visher J L and Sievenpiper D F 2010 Scalar and tensor holographic artificial impedance surfaces *IEEE Trans. Antennas Propag.* **58** 3212–21
[32] Holloway C L, Kuester E F, Gordon J A, O'Hara J, Booth J and Smith D R 2012 An overview of the theory and applications of metasurfaces: the two-dimensional equivalents of metamaterials *IEEE Antennas Propag. Mag.* **54** 10–35
[33] Pfeiffer C and Grbic A 2013 Metamaterial Huygens' surfaces: tailoring wave fronts with reflectionless sheets *Phys. Rev. Lett.* **110** 197401
[34] Selvanayagam M and Eleftheriades G V 2013 Discontinuous electromagnetic fields using orthogonal electric and

magnetic currents for wavefront manipulation *Opt. Express* **21** 14409–29
[35] Wong J P S, Epstein A and Eleftheriades G V 2015 Reflectionless wide-angle refracting metasurfaces *IEEE Antennas Wireless Propag. Lett.* **15** 1293–6
[36] Chen M, Abdo-Sanchez E, Epstein A and Eleftheriades G V 2018 Theory, design, and experimental verification of reflectionless bianisotropic Huygens' metasurface for wide angle refraction *Phys. Rev.* B **97** 125433
[37] Epstein A and Eleftheriades G V 2016 Arbitrary power conserving field transformations with passive lossless Omega-type bianisotropic metasurfaces *IEEE Trans. Antennas Propag.* **64** 3880–95
[38] Epstein A, Wong J P S and Eleftheriades G V 2016 Cavity-excited Huygens' metasurface antennas for near-unity aperture efficiency from arbitrarily large apertures *Nat. Commun.* **7** 10360
[39] Chen M, Epstein A, Eleftheriades G V and Huygens' Metasurface A 2018 A Huygens' metasurface lens for enhancing the gain of frequency-scanned slotted waveguide antennas *URSI National Radio Science Meeting (Boulder, CO)*
[40] Epstein A and Eleftheriades G V 2017 Arbitrary antenna arrays without feed networks based on cavity-excited omega-bianisotropic metasurfaces *IEEE Trans. Antennas Propag.* **65** 1749–56
[41] Dorrah A H and Eleftheriades G V 2018 Bianisotropic Huygens' metasurface pairs for nonlocal power-conserving wave transformations *IEEE Antennas Wireless Propag. Lett.* **17** 1788–92
[42] Dorrah A and Eleftheriades G V 2018 All-pass characteristics of a Huygens' unit cell *URSI National Radio Science Meeting (Boulder, CO)*
[43] Cameron T R and Eleftheriades G V 2017 Experimental validation of a wideband metasurface for wide-angle scanning leaky-wave antennas *IEEE Trans. Antennas Propag.* **65** 5245–56
[44] Bomzon Z, Biener G, Kleiner V and Hasman E 2002 Radially and azimuthally polarized beams generated by space-variant dielectric subwavelength gratings *Opt. Lett.* **27** 285–7
[45] Schwanecke A, Krasavin A, Bagnall D M, Potts A, Zayats A V and Zheludev N I 2003 Broken time reversal of light interaction with of planar chiral nanostructures *Phys. Rev. Lett.* **91** 247404
[46] Hasman E, Kleiner V, Biener G and Niv A 2003 Polarization dependent focusing lens by use of quantized Pancharatnam-Berry phase diffractive optics *Appl. Phys. Lett.* **82** 328–30
[47] Fedotov V A, Wallauer J, Walther M, Perino M, Papasimakis N and Zheludev N I 2015 Wavevector selective metasurfaces and tunnel vision filters *Light Sci. Appl.* **4** e306
[48] Yu N, Genevet P, Kats M A, Aieta F, Tetienne J-P and Capasso F 2011 Light propagation with phase discontinuities: generalized laws of reflection and refraction *Science* **334** 333–7
[49] Khorasaninejad M, Chen W T, Devlin R C, Oh J, Zhu A Y and Capasso F 2016 Metalenses at visible wavelengths: diffraction-limited focusing and subwavelength resolution imaging *Science* **352** 1190–4
[50] Yuan G H, Rogers E T F and Zheludev N I 2018 'Plasmonics' in free space: observation of giant wavevectors, vortices and energy backflow in superoscillatory optical fields *Light Sci. Appl.* **8** 2
[51] Papasimakis N, Fedotov V A, Savinov V, Raybould T A and Zheludev N I 2016 Electromagnetic toroidal excitations in matter and free space *Nat. Mater.* **15** 263–71
[52] Papasimakis N, Raybould T A, Fedotov V A, Tsai D P, Youngs I and Zheludev N I 2018 Pulse generation scheme for flying electromagnetic doughnuts *Phys. Rev.* B **97** 201409
[53] Zdagkas A, Moitra P, Buchnev O, Papasimakis N and Zheludev N I 2018 Launching electromagnetic donuts: non-transverse electromagnetic pulses *CLEO 2018 (San Jose, CA, 13–18 May 2018)*
[54] Holloway C L, Kuester E F, Gordon J A, O'Hara J, Booth J and Smith D R 2012 An overview of the theory and applications of metasurfaces: the two-dimensional equivalents of metamaterials *IEEE Antennas Propag. Mag.* **54** 10–35
[55] Kildishev A V, Boltasseva A and Shalaev V M 2013 Planar photonics with metasurfaces *Science* **339** 1232009
[56] Yu N, Genevet P, Aieta F, Kats M A, Blanchard R, Aoust G, Tetienne J-P, Gaburro Z and Capasso F 2013 Flat optics: controlling wavefronts with optical antenna metasurfaces *IEEE J. Sel. Top. Quantum Electron.* **19** 4700423
[57] Yu N and Capasso F 2014 Flat optics with designer metasurfaces *Nat. Mater.* **13** 139–50
[58] Walia S, Shah C M, Gutruf P, Nili H, Chowdhury D R, Withayachumnankul W, Bhaskaran M and Sriram S 2015 Flexible metasurfaces and metamaterials: a review of materials and fabrication processes at micro- and nano-scales *Appl. Phys. Rev.* **2** 011303
[59] Minovich A E, Miroshnichenko A E, Bykov A Y, Murzina T V, Neshev D N and Kivshar Y S 2015 Functional and nonlinear optical metasurfaces *Laser Photon. Rev.* **9** 195–213
[60] Genevet P and Capasso F 2015 Holographic optical metasurfaces: a review of current progress *Rep. Prog. Phys.* **78** 024401
[61] Chen H-T, Taylor A J and Yu N 2016 A review of metasurfaces: physics and applications *Rep. Prog. Phys.* **79** 076401
[62] Hsiao H-H, Chu C H and Tsai D P 2017 Fundamentals and applications of metasurfaces *Small Methods* **1** 1600064
[63] Meinzer N, Barnes W L and Hooper I R 2014 Plasmonic meta-atoms and metasurfaces *Nat. Photonics* **8** 889–98
[64] Glybovski S B, Tretyakov S A, Belov P A, Kivshar Y S and Simovski C R 2016 Metasurfaces: from microwaves to visible *Phys. Rep.* **634** 1–72
[65] Zhu A Y, Kuznetsov A I, Luk'yanchuk B, Engheta N and Genevet P 2017 Traditional and emerging materials for optical metasurfaces *Nanophotonics* **6** 452–71
[66] Choudhury S M, Wang D, Chaudhuri K, DeVault C, Kildishev A V, Boltasseva A and Shalaev V M 2018 Material platforms for optical metasurfaces *Nanophotonics* (https://doi.org/10.1515/nanoph-2017-0130)
[67] Fan S 2014 Photovoltaics: an alternative 'Sun' for solar cells *Nat. Nanotechnol.* **9** 92–3
[68] Shockley W and Queisser H J 1961 Detailed balance limit of efficiency of p-n Junction solar cells *J. Appl. Phys.* **32** 510–9
[69] Lenert A, Bierman D M, Nam Y, Chan W R, Celanović I, Soljačić M and Wang E N 2014 A nanophotonic solar thermophotovoltaic device *Nat. Nanotechnol.* **9** 126–30
[70] Fraas L and Minkin L 2007 TPV history from 1990 to present and future trends *AIP Conf. Proc.* **890** 17–23
[71] Chan W R, Bermel P, Pilawa-Podgurski R C N, Marton C H, Jensen K F, Senkevich J J, Joannopoulos J D, Soljacic M and Celanovic I 2013 Toward high-energy-density, high-efficiency, and moderate-temperature chip-scale thermophotovoltaics *Proc. Natl. Acad. Sci.* **110** 5309–14
[72] Fraas L M and Strauch J 2010 Design and thermal modeling of a portable fuel fired cylindrical TPV battery replacement *Thesis* Sandia National Laboratories
[73] Aydin K, Ferry V E, Briggs R M and Atwater H A 2011 Broadband polarization-independent resonant light absorption using ultrathin plasmonic super absorbers *Nat. Commun.* **2** 517

[74] Bermel P, Soljacic M and Celanovic I 2011 Thermophotovoltaic power conversion systems: current performance and future potential *Chem. Business* **28** 56
[75] Karalis A and Joannopoulos J D 2016 'Squeezing' near-field thermal emission for ultra-efficient high-power thermophotovoltaic conversion *Sci. Rep.* **6** 28472
[76] Li W, Guler U, Kinsey N, Naik G V, Boltasseva A, Guan J, Shalaev V M and Kildishev A V 2014 Refractory plasmonics with titanium nitride: broadband metamaterial absorber *Adv. Mater.* **26** 7959–65
[77] Albrecht G, Kaiser S, Giessen H and Hentschel M 2017 Refractory plasmonics without refractory materials *Nano Lett.* **17** 6402–8
[78] Parmigiani F, Scagliotti M, Samoggia G and Ferraris G P 1985 Influence of the growth conditions on the optical properties of thin gold films *Thin Solid Films* **125** 229–34
[79] Shemelya C, DeMeo D, Latham N P, Wu X, Bingham C, Padilla W and Vandervelde T E 2014 Stable high temperature metamaterial emitters for thermophotovoltaic applications *Appl. Phys. Lett.* **104** 201113
[80] Zhao B, Wang L, Shuai Y and Zhang Z M 2013 Thermophotovoltaic emitters based on a two-dimensional grating/thin-film nanostructure *Int. J. Heat Mass Transf.* **67** 637–45
[81] Ghanekar A, Lin L and Zheng Y 2016 Novel and efficient Mie-metamaterial thermal emitter for thermophotovoltaic systems *Opt. Express* **24** A868
[82] Guler U, Boltasseva A and Shalaev V M 2014 Refractory plasmonics *Science* **344** 263–4
[83] Reddy H, Guler U, Kudyshev Z, Kildishev A V, Shalaev V M and Boltasseva A 2017 Temperature-dependent optical properties of plasmonic titanium nitride thin films *ACS Photonics* **4** 1413–20
[84] Guler U, Ndukaife J C, Naik G V, Nnanna A G A, Kildishev A V, Shalaev V M and Boltasseva A 2013 Local heating with lithographically fabricated plasmonic titanium nitride nanoparticles *Nano Lett.* **13** 6078–83
[85] Hu J, Ren X, Reed A N, Reese T, Rhee D, Howe B, Lauhon L J, Urbas A M and Odom T W 2017 Evolutionary design and prototyping of single crystalline titanium nitride lattice optics *ACS Photonics* **4** 606–12
[86] Chaudhuri K, Shaltout A, Guler U, Shalaev V M and Boltasseva A 2016 High efficiency phase gradient metasurface using refractory plasmonic zirconium nitride *Conf. on Lasers and Electro-Optics* (Washington, DC: Optical Society of America) p FM3N.2
[87] Coppens Z J, Kravchenko I I and Valentine J G 2016 Lithography-free large-area metamaterials for stable thermophotovoltaic energy conversion *Adv. Opt. Mater.* **4** 671–6
[88] Woolf D N, Kadlec E A, Bethke D, Grine A D, Nogan J J, Cederberg J G, Bruce Burckel D, Luk T S, Shaner E A and Hensley J M 2018 High-efficiency thermophotovoltaic energy conversion enabled by a metamaterial selective emitter *Optica* **5** 213
[89] Guler U, Kildishev A, Shalaev V M, Boltasseva A and Naik G 2015 Refractory plasmonic metamaterial absorber and emitter for energy harvesting *US Patent Specification* US2015 0288318A1
[90] Sievenpiper D, Schaffner J, Song H, Loo R and Tangonan G 2003 Two-dimensional beam steering using an electrically tunable impedance surface *IEEE Trans. Antennas Propag.* **51** 2713–22
[91] Kim S, Wakatsuchi H, Rushton J and Sievenpiper D 2016 Switchable nonlinear metasurfaces for absorbing high power surface waves *Appl. Phys. Lett.* **108** 041903
[92] Li A, Kim S, Luo Y, Li Y, Long J and Sievenpiper D 2017 High-power, transistor-based tunable and switchable metasurface absorber *IEEE Trans. Microw. Theory Tech.* **65** 2810–8
[93] Wakatsuchi H, Kim S, Rushton J J and Sievenpiper D 2013 Waveform-dependent absorbing metasurfaces *Phys. Rev. Lett.* **111** 245501
[94] Kim S 2017 Nonlinear active metamaterial surfaces *PhD Thesis* University of California San Diego
[95] Rozanov K 2000 Ultimate thickness to bandwidth ratio of radar absorbers *IEEE Trans. Antennas Propag.* **48** 1230
[96] Luo Z, Chen X, Long J, Quarfoth R and Sievenpiper D 2015 Self-focusing of electromagnetic surface waves on a nonlinear impedance surface *Appl. Phys. Lett.* **106** 211102
[97] Hrabar S, Krois I, Bonic I and Kiricenko A 2011 Negative capacitor paves the way to ultra-broadband metamaterials *Appl. Phys. Lett.* **99** 254103
[98] Long J and Sievenpiper D F 2016 Low-profile and low-dispersion artificial impedance surface in the UHF band based on non-foster circuit loading *IEEE Trans. Antennas Propag.* **64** 3003–10
[99] Piltan S and Sievenpiper D 2018 Field enhancement in plasmonic nanostructures *J. Opt.* **20** 055401
[100] Forati E, Dill T, Tao A and Sievenpiper D 2016 Photoemission-based microelectronic devices *Nat. Commun.* **7** 13399
[101] Couch A and Grbic A 2016 A phase-tunable liquid crystal-based metasurface *10th Int. Congress on Advanced Electromagnetic Materials in Microwaves and Optics (METAMATERIALS)* pp 94–6
[102] Cure D, Weller T, Price T, Miranda F and Van Keuls F 2014 Low-profile tunable dipole antenna using barium strontium titanate varactors *IEEE Trans. Antennas Propag.* **62** 1185–93
[103] Kahmen G and Schumacher H 2017 Interactive design of MEMS varactors with high accuracy and application in an ultralow noise MEMS-based RF VCO *IEEE Trans. Microw. Theory Tech.* **65** 3578–84
[104] Caloz C, Alù A, Tretyakov S, Sounas D L, Achouri K and Deck-Léger Z-L 2018 Electromagnetic nonreciprocity *Phys. Rev. Appl.* **10** 047001
[105] Jackson J D 1998 *Classical Electrodynamics* (New York: Wiley)
[106] Martin T (ed) 1933 *Faraday's Diary* (George Bell and Sons) IV (1839–1847)
[107] Onsager L 1931 Reciprocal relations in irreversible processes I *Phys. Rev.* **37** 405–26
Onsager L 1938 Reciprocal relations in irreversible processes II *Phys. Rev.* **38** 2265–79
[108] Caloz C and Alù A 2018 Magnet-less nonreciprocity in electromagnetics *IEEE Antennas Wireless Compon. Lett.* **17** 1931–7
[109] Parsa A, Kodera T and Caloz C 2011 Ferrite based non-reciprocal radome, generalized scattering matrix analysis and experimental demonstration *IEEE Trans. Antennas Propag.* **59** 810–7
[110] Kodera T, Sounas D L and Caloz C 2010 Artificial Faraday rotation using a ring metamaterial structure without static magnetic field *Appl. Phys. Lett.* **99** 031114
[111] Kodera T, Sounas D L and Caloz C 2013 Magnetless non-reciprocal metamaterial (MNM) technology: application to microwave components *IEEE Trans. Microw. Theory Tech.* **61** 1030–42
[112] Kodera T, Sounas D L and Caloz C 2012 Non-reciprocal magnet-less CRLH leaky-wave antenna based on a ring metamaterial structure *IEEE Antennas Wireless Propag. Lett.* **10** 1551–4
[113] Wang Z, Wang Z, Wang J, Zhang B, Huangfu J, Joannopoulos J D, Soljačić M and Rana L 2012 Gyrotropic response in the absence of a bias field *Proc. Natl Acad. Sci.* **109** 13194–7

[114] Caloz C and Deck-Léger Z-L 2019 Spacetime metamaterials arXiv:1905.00560
[115] Taravati S, Khan B S, Gupta S, Achouri K and Caloz C 2017 Nonreciprocal nongyrotropic magnetless metasurface *IEEE Trans. Antennas Propag.* **65** 3589–97
[116] Hadad Y, Sounas D L and Alù A 2015 Space-time gradient metasurfaces *Phys. Rev.* B **92** 100304
[117] Shaltout A, Kildishev A and Shalaev V 2015 Time-varying metasurface and Lorentz nonreciprocity *Opt. Mat. Express* **5** 2459–67
[118] Shi Y, Han S and Fan S 2017 Optical circulation and isolation based on indirect photonic transitions of guided resonance modes *ACS Photonics* **4** 1639–45
[119] Zang R, Caloz C and Zhang Q 2015 Relay multiplexing enhancement using a nonreciprocal antenna array *IEEE Int. Symp. Antennas Propag (ISAP)* pp 271–3
[120] Radi Y and Alù A 2018 Reconfigurable metagratings *ACS Photonics* **5** 1779–85
[121] Chen K *et al* 2017 A reconfigurable active Huygens' metalens *Adv. Mater.* **29** 1606422
[122] Zhao X, Schalch J, Zhang J, Seren H R, Duan G, Averitt R D and Zhang X 2018 Electromechanically tunable metasurface transmission waveplate at terahertz frequencies *Optica* **5** 303–10
[123] Karvounis A, Gholipour B, MacDonald K F and Zheludev N I 2016 All-dielectric phase-change reconfigurable metasurface *Appl. Phys. Lett.* **109** 051103
[124] Chen P Y, Argyropoulos C and Alù A 2013 Broadening the cloaking bandwidth with non-Foster metasurfaces *Phys. Rev. Lett.* **111** 233001
[125] Hadad Y, Sounas D L and Alù A 2015 Space-time gradient metasurfaces *Phys. Rev.* B **92** 100304R
[126] Regensburger A, Bersch C, Miri M A, Onishchukov G, Christodoulides D N and Peschel U 2012 Parity-time synthetic photonic lattices *Nature* **488** 167–71
[127] Monticone F, Valagiannopoulos C A and Alù A 2016 Aberration-free imaging based on parity-time symmetric nonlocal metasurfaces *Phys. Rev.* X **6** 041018
[128] Fleury F, Sounas D L and Alù A 2015 An invisible acoustic sensor based on parity-time symmetry *Nat. Commun.* **6** 5905
[129] Sounas D L, Fleury R and Alù A 2015 Unidirectional cloaking based on metasurfaces with balanced loss and gain *Phys. Rev. Appl.* **4** 014005
[130] Chen H-T, Padilla W J, Zide J M O, Gossard A C, Taylor A J and Averitt R D 2006 Active terahertz metamaterial devices *Nature* **444** 597–600
[131] Zhu B, Feng Y, Zhao J, Huang C and Jiang T 2010 Switchable metamaterial reflector/absorber for different polarized electromagnetic waves *Appl. Phys. Lett.* **97** 2010–2
[132] Chen H-T, Padilla W J, Cich M J, Azad A K, Averitt R D and Taylor A J 2009 A metamaterial solid-state terahertz phase modulator *Nat. Photonics* **3** 148–51
[133] Lee S H *et al* 2012 Switching terahertz waves with gate-controlled active graphene metamaterials *Nat. Mater.* **11** 936–41
[134] Sautter J, Staude I, Decker M, Rusak E, Neshev D N, Brener I and Kivshar Y S 2015 Active tuning of all-dielectric metasurfaces *ACS Nano* **9** 4308–15
[135] Chen H-T, O'Hara J F, Azad A K, Taylor A J, Averitt R D, Shrekenhamer D B and Padilla W J 2008 Experimental demonstration of frequency-agile terahertz metamaterials *Nat. Photonics* **2** 295–8
[136] Ou J-Y, Plum E, Zhang J and Zheludev N I 2013 An electromechanically reconfigurable plasmonic metamaterial operating in the near-infrared *Nat. Nanotechnol.* **8** 252–5
[137] Miao Z, Wu Q, Li X, He Q, Ding K, An Z, Zhang Y and Zhou L 2015 Widely tunable terahertz phase modulation with gate-controlled graphene metasurfaces *Phys. Rev.* X **5** 041027
[138] Sievenpiper D F, Schaffner J H, Song H J, Loo R Y and Tangonan G 2003 Two-dimensional beam steering using an electrically tunable impedance surface *IEEE Trans. Antennas Propag.* **51** 2713–22
[139] Xu H-X, Sun S, Tang S, Ma S, He Q, Wang G-M, Cai T, Li H-P and Zhou L 2016 Dynamical control on helicity of electromagnetic waves by tunable metasurfaces *Sci. Rep.* **6** 27503
[140] She A, Zhang S, Shian S, Clarke D R and Capasso F 2018 Adaptive metalenses with simultaneous electrical control of focal length, astigmatism, and shift *Sci. Adv.* **4** eaap9957
[141] Xu H-X, Ma S, Luo W, Cai T, Sun S, He Q and Zhou L 2016 Aberration-free and functionality-switchable meta-lenses based on tunable metasurfaces *Appl. Phys. Lett.* **109** 193506
[142] Li L, Jun Cui T, Ji W, Liu S, Ding J, Wan X, Bo Li Y, Jiang M, Qiu C and Zhang S 2017 Electromagnetic reprogrammable coding-metasurface holograms *Nat. Commun.* **8** 197
[143] Watts C M, Shrekenhamer D, Montoya J, Lipworth G, Hunt J, Sleasman T, Krishna S, Smith D R and Padilla W J 2014 Terahertz compressive imaging with metamaterial spatial light modulators *Nat. Photonics* **8** 605–9
[144] Huang Y-W, Lee H W H, Sokhoyan R, Pala R A, Thyagarajan K, Han S, Tsai D P and Atwater H A 2016 Gate-tunable conducting oxide metasurfaces *Nano Lett.* **16** 5319–25
[145] Qu C *et al* 2015 Tailor the functionalities of metasurfaces based on a complete phase diagram *Phys. Rev. Lett.* **115** 235503
[146] Mostafazadeh A 2009 Spectral singularities of complex scattering potentials and infinite reflection and transmission coefficients at real energies *Phys. Rev. Lett.* **102** 220402
[147] Mock A 2016 Parity-time–symmetry breaking in two-dimensional photonic crystals: square lattice *Phys. Rev.* A **93** 063812
[148] Lu L, Joannopoulos J D and Soljačić M 2014 Topological photonics *Nat. Photon.* **8** 821–9
[149] Hessel A, Chen M H, Li R C M and Oliner A A 1973 Propagation in periodically loaded waveguides with higher symmetries *Proc. IEEE* **61** 183–95
[150] Valerio G, Ghasemifard F, Sipus Z and Quevedo-Teruel O 2018 Glide-symmetric all-metal holey metasurfaces for low-dispersive artificial materials: modeling and properties *IEEE Trans. Microw. Theory Tech.* **66** 3210–23
[151] Dahlberg O, Mitchell-Thomas R and Quevedo-Teruel O 2017 Reducing the dispersion of periodic structures with twist and polar glide symmetries *Sci. Rep.* **7** 10136
[152] Bagheriasl M and Valerio G 2019 Bloch analysis of electromagnetic waves in twist-symmetric lines *Symmetry* **11** 620
[153] Quevedo-Teruel O, Ebrahimpouri M and Ng Mou Kehn M 2016 Ultrawideband metasurface lenses based on off-shifted opposite layers *IEEE Antennas and Wireless Propagation Letters* **15** 484–7
[154] Ebrahimpouri M, Rajo-Iglesias E, Sipus Z and Quevedo-Teruel O 2018 Cost-effective gap waveguide technology based on glide-symmetric holey EBG structures *IEEE Trans. Microw. Theory Tech.* **66** 927–34
[155] Valerio G, David R, Jackson D R and Galli A 2010 Fundamental properties of surface waves in lossless stratified structures *Proc. R. Soc.* A **466** 2447–69
[156] Valerio G, Sipus Z, Grbic A and Quevedo-Teruel O 2017 Accurate equivalent-circuit descriptions of thin glide-symmetric corrugated metasurfaces *IEEE Trans. Antennas Propag.* **65** 2695–700
[157] Valerio G, Paulotto S, Baccarelli P, Burghignoli P and Galli A 2011 Accurate Bloch analysis of 1D periodic lines

through the simulation of truncated structures *IEEE Trans Antennas Progag.* **59** 2188–95
[158] Bagheriasl M, Quevedo-Teruel O and Valerio G 2019 Bloch analysis of artificial lines and surfaces exhibiting glide symmetry *IEEE Trans. Microw. Theory Tech.* pp 1–11
[159] Mesa F, Rodríguez-Berral R and Medina F 2018 On the computation of the dispersion diagram of symmetric one-dimensionally periodic structures *Symmetry* **10** 307
[160] Figotin A and Vitebskiy I 2003 Oblique frozen modes in periodic layered media *Phys. Rev.* E **68** 036609
[161] Mohammad H, Zheng T, Casaletti C, Ren Z, Abdelshafy A F, Capolino F and Valerio G 2018 Degenerate band edge condition in substrate-integrated waveguides *Antennas Propag. Int. Symp. (Boston, MA, 8–13 July 2018)*
[162] Kildal P-S, Alfonso E, Valero-Nogueira A and Rajo-Iglesias E 2009 Local metamaterial based waveguides in gaps between parallel metal plates *IEEE Antennas Wireless Propag. Lett.* **8** 84–9
[163] Kildal P-S, Zaman A U, Rajo-Iglesias E, Alfonso E and Valero-Nogueira A 2011 Design and experimental verification of ridge gap waveguide in bed of nails for parallel-plate mode suppression *IET Microwaves Antennas Propag.* **5** 262–70
[164] Fan F, Yang J, Vassilev V and Zaman A U 2018 Bandwidth investigation of half-height pin in ridge gap waveguide *IEEE Trans. Microw. Theory Tech.* **66** 100–8
[165] Pucci E, Rajo-Iglesias E and Kildal P-S 2012 New microstrip gap waveguide on mushroom-type EBG for packaging of microwave components *IEEE Microwave Wireless Comp. Lett.* **222** 129–31
[166] Sharfi Sorkherizi M and Kishk A A 2016 Fully printed gap waveguide with facilitated design properties *IEEE Microwave Wireless Comp. Lett.* **26** 657–9
[167] Ebrahimpouri M, Quevedo-Teruel O and Rajo-Iglesias E 2017 Design guidelines for gap waveguide technology based on glide-symmetric holey structures *IEEE Microwave Wireless Comp. Lett.* **27** 542–4
[168] Rajo-Iglesias E, Ebrahimpouri M and Quevedo-Teruel O 2018 Wideband phase shifter in groove gap wavelength technology implemented with glide-symmetric holey EBG *IEEE Microwave Wireless Comp. Lett.* **28** 476–8
[169] Ebrahimpouri M, Algaba Brazalez A, Manholm L and Quevedo-Teruel O 2018 Using glide-symmetric holes to reduce leakage between waveguide flanges *IEEE Microwave Wireless Comp. Lett.* **28** 473–5
[170] Rajo-Iglesias E and Kildal P-S 2010 Groove gap waveguide: a rectangular waveguide between contactless metal plates enabled by parallel-plate cut-off *Proc. 4th European Conf. on Antennas and Propagation (Barcelona, Spain)*
[171] Crepeau P-J and McIsaac P-R 1964 Consequences of symmetry in periodic structures *Proc. IEEE* **52** 33–43
[172] Quevedo-Teruel O, Miao J, Mattsson M, Algaba-Brazalez A, Johansson M and Manholm L 2018 Glide-symmetric fully-metallic Luneburg lens for 5G communications at Ka-band *IEEE Antennas Wireless Propag. Lett.* **17** 1588–92
[173] Camacho-Aguilar M, Mitchell-Thomas R, Hibbins A P, Sambles J R and Quevedo-Teruel O 2017 Mimicking glide symmetry dispersion with couple slot metasurfaces *Appl. Phys. Lett.* **111** 121603
[174] Chen Q, Ghasemifard F, Valerio G and Quevedo-Teruel O 2018 Modeling and dispersion analysis of coaxial lines with higher symmetries *IEEE Trans. Microw. Theory Tech.* **66** 4338–45
[175] Ghasemifard F, Norgren M and Quevedo-Teruel O 2018 Dispersion analysis of 2D glide-symmetric corrugated metasurfaces using mode-matching technique *IEEE Microwave Wireless Comp. Lett.* **28** 1–3
[176] Ghasemifard F, Norgren M, Quevedo-Teruel O and Valerio G 2018 Analyzing glide-symmetric holey metasurfaces using a generalized Floquet theorem *IEEE Access* **6** 71743–50
[177] Grbic A and Eleftheriades G 2003 Periodic analysis of a 2D negative refractive index transmission line structure *IEEE Trans. Antennas Propag.* **51** 2604–11
[178] Munk B 2000 *Frequency Selective Surfaces: Theory and Design* (New York: Wiley)
[179] Huang J and Encinar J A 2007 *Reflectarray Antennas* (Hoboken, NJ: Wiley)
[180] Marcuvitz N 1951 *Waveguide Handbook* (New York: McGraw-Hill)
[181] Palocz I and Oliner A A 1970 Equivalent network of a multimode planar grating *IEEE Trans. Microw. Theory Techn.* **18** 244–52
[182] Dubrovka R, Vazquez J, Parini C and Moore D 2006 Equivalent circuit method for analysis and synthesis of frequency selective surfaces *IET Proc. Microwaves Antennas Propag.* **153** 213–20
[183] Mesa F, Rodríguez-Berral R and Medina F 2018 Unlocking complexity with ECA. The equivalent circuit model as an efficient and physically insightful tool for microwave engineering *IEEE Microwave Magazine* **19** 44–65
[184] Kurokawa K 1969 *An Introduction to the Theory of Microwave Circuits* (New York: Academic)
[185] Mesa F *et al* 2015 Circuit-model analysis of frequency selective surfaces with scatterers of arbitrary geometry *IEEE Antennas Wireless Propag. Lett.* **14** 135–8
[186] Costa F, Monorchio A and Manara G 2012 Efficient analysis of frequency-selective surfaces by a simple equivalent-circuit model *IEEE Antennas Propag. Mag.* **54** 35–48
[187] Tao H *et al* 2008 Terahertz metamaterials on free-standing highly flexible polyimide substrates *J. Phys. D: Appl. Phys.* **41** 232004
[188] Asadchy V, Díaz-Rubio A and Tretyakov S 2018 Bianisotropic metasurfaces: physics and applications *Nanophotonics* (https://doi.org/10.1515/nanoph-2017-0132)
[189] Asadchy V, Díaz-Rubio A, Kwon D-H and Tretyakov S 2019 Analytical modeling of electromagnetic surfaces *Surface Electromagnetics with Applications in Antenna, Microwave, and Optical Engineering* ed F Yang and Y Rahmat-Samii (Cambridge: Cambridge University Press)
[190] Asadchy V, Díaz-Rubio A, Tcvetkova S, Kwon D-H, Elsakka A, Albooyeh M and Tretyakov S 2017 Flat engineered multichannel reflectors *Phys. Rev.* X **7** 031046
[191] Díaz-Rubio A, Asadchy V, Elsakka A and Tretyakov S 2017 From the generalized reflection law to the realization of perfect anomalous reflectors *Sci. Adv.* **3** e1602714
[192] Ra'di Y, Sounas D and Alu A 2017 Metagratings: beyond the limits of graded metasurfaces for wave front control *Phys. Rev. Lett.* **119** 067404
[193] Epstein A and Rabinovich O 2017 Unveiling the properties of metagratings via a detailed analytical model for synthesis and analysis *Phys. Rev. Appl.* **8** 054037
[194] Epstein A and Eleftheriades G V 2016 Arbitrary power-conserving field transformations with passive lossless omega-type bianisotropic metasurfaces *IEEE Trans. Antennas Propag.* **64** 3880–95
[195] Díaz-Rubio A, Li J, Shen C, Cummer S and Tretyakov S 2018 Power-flow conformal metamirrors for engineering wave reflections *Sci. Adv.* **5** eaau7288
[196] Taravati S and Caloz C 2017 Mixer-duplexer-antenna leaky-wave system based on periodic space-time modulation *IEEE Trans. Antennas Propag.* **65** 442–52
[197] Stewart S A, Smy T J and Gupta S 2018 Finite-difference time-domain modeling of space–time-modulated metasurfaces *IEEE Trans. Antennas Propag.* **66** 282–92

[198] Shi Y, Han S and Fan S 2017 Optical circulation and isolation based on indirect photonic transitions of guided resonance modes *ACS Photonics* **4** 1639–45
[199] Michalski K and Mosig J 1997 Multilayered media Green's functions in integral equation formulations *IEEE Trans. Antennas Propag.* **45** 508–19
[200] Kuester E, Mohamed M, Piket-May M and Holloway C 2003 Averaged transition conditions for electromagnetic fields at a metafilm *IEEE Trans. Antennas Propag.* **51** 2641–51
[201] Chamanara N, Achouri K and Caloz C 2017 Efficient analysis of metasurfaces in terms of spectral-domain GSTC integral equations *IEEE Trans. Antennas Propag.* **65** 5340–7
[202] Francavilla M, Martini E, Maci S and Vecchi G 2015 On the numerical simulation of metasurfaces with impedance boundary conditions *IEEE Trans. Antennas Propag.* **63** 2153–61
[203] Craeye C, Radu X, Capolino F and Schuchinsky A 2009 Fundamentals of method of moments for articifical materials *Theory and Phenomena of Metamaterials* (Boca Raton, FL: CRC Press)
[204] Vahabzadeh Y, Chamanara N, Achouri K and Caloz C 2017 Computational analysis of metasurfaces *IEEE J. Multiscale Multiphysics Comp. Techn.* **3** 37–49
[205] Gonzalez-Ovejero D and Maci S 2015 Gaussian ring functions for the analysis of modulated metausrface antennas *IEEE Trans. Antennas Propag.* **63** 3982–93
[206] Bodehou M, González-Ovejero D, Craeye C and Huynen I 2019 Method of moments simulation of modulated metasurface antennas with a set of orthogonal entire-domain basis functions *IEEE Trans. Antennas Propag.* **67** 1119–30
[207] Bodehou M, Craeye C and Huynen I 2018 Fourier-Bessel basis functions for the analysis of elliptical domain metasurface antennas *IEEE Antenna Wireless Propag. Lett.* **17** 675–8
[208] Bodehou M, Craeye C, Martini M and Huynen I 2019 A quasi-direct method for the surface impedance design of modulated metasurface antennas *IEEE Trans. Antennas Propag.* **67** 24–36
[209] De Vita P, Freni A, Pirinoli P and Vecchi G 2006 Fast analysis of large finite arrays with a combined multiresolution—SM/AIM approach *IEEE Trans. Antennas Propag.* **54** 3827–32
[210] Suter E and Mosig J 2000 A subdomain multilevel approach for the efficient MoM analysis of large planar antennas *Microw. Opt. Technol. Lett.* **26** 280–7
[211] Okhmatovski V, Yuan M, Jeffrey I and Phelps R 2009 A three-dimentional precorrected FFT algorithm for fast method of moments solutions of the mixed-potential integral equation in layered media *IEEE Trans. Microw. Theory Techn.* **57** 3505–17
[212] Ginste D, Michielssen E, Olyslager F and De Zutter D 2006 An efficient perfectly matched layer based multilevel fast multipole algorithm for large planar microwave structures *IEEE Trans. Antennas Propag.* **54** 1538–48
[213] Maci S and Cucini A 2006 FSS-based EBG metasurfaces *Metamaterials: Physics and Engineering Explorations* ed N Engheta and R Ziolkowski (Piscataway, NJ: IEEE)